Article

Molecular structure and photoinduced intramolecular hydrogen bonding in 2-pyrrolylmethylidene cycloalkanones

Mark Sigalov, Bagrat A. Shainyan, Nina N. Chipanina, Larisa P. Oznobikhina, Natalia Strashnikova, and Irina Sterkhova

J. Org. Chem., **Just Accepted Manuscript** • DOI: 10.1021/acs.joc.5b01604 • Publication Date (Web): 12 Oct 2015

Molecular structure and photoinduced intramolecular hydrogen bonding in 2-pyrrolylmethylidene cycloalkanones

Mark Sigalov,*[a)] Bagrat Shainyan,[b)] Nina Chipanina,[b)] Larisa Oznobikhina,[b)] Natalia Strashnikova [a)], Irina Sterkhova[b)]

[a)] *Department of Chemistry, Ben-Gurion University of the Negev, 84105 Beer-Sheva, Israel*, msigalov@bgu.ac.il

[b)] *A.E. Favorsky Irkutsk Institute of Chemistry, Siberian Division of Russian Academy of Sciences, 664033 Irkutsk, Russia*

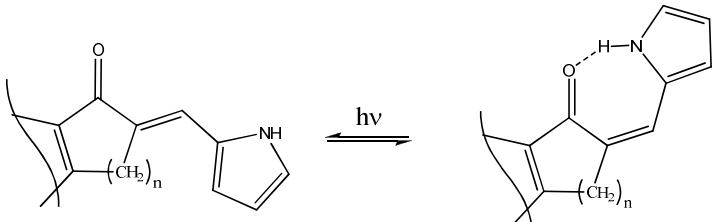

E **Z**

Abstract

The structure of pyrrolylmethylidene derivatives of 2,3-dihydro-1H-inden-1-one (**3**) , 3,4-dihydro-naphthalen-1(2H)-one (**4**) and cycloalkanones (**5**–**7**) was studied at the first time in solid state and in solution by NMR, IR and UV spectroscopy supported by DFT quantum mechanical calculations. It was shown that all studied compounds except cycloheptanone derivative **7** both in crystal and in solution exist in the form of dimers where single E- or E,E-configuration with respect to the exocyclic C=C bond is stabilized

by intermolecular hydrogen bonds N-H···O=C. UV-irradiation at wavelength 365 nm of MeCN or DMSO solutions of **3**-**6** results, depending on the exposition time and solvent, in partial to complete isomerization to the Z- or Z,E-isomers (in the case of **6**, also the Z,Z-isomer). The NMR and IR spectroscopy data show the existence of a strong intramolecular hydrogen bond N-H···O=C in the Z-moieties of isomerized compounds. The studied compounds are protonated by trifluoroacetic acid at the carbonyl oxygen, in spite of the reverse order of basicity and nucleophilicity of the carbonyl group and the pyrrole ring. Investigation of the behavior of compound **6** with respect to acetate and fluoride anions allows to consider it as perspective fluoride sensor.

INTRODUCTION

Chemistry of chalcones including their cyclic analogs **1** and cross-conjugated α, α'-bis-(arylmethylidene) derivatives of cyclic ketones (dienones) **2** is an extensively growing area at present time. Numerous representatives of these classes of unsaturated compounds have a vast field of applications in biology, medicine, optics, rocket engineering and as building blocks in the synthesis of heterocyclic compounds and thermostable polymeric materials[1–18]. Their methods of synthesis, structure, physico-chemical properties and characteristic reactions are summarized in the recent review [19].

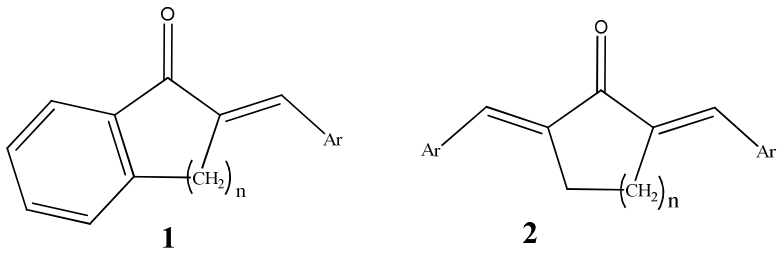

n = 1-3; Ar = X-C_6H_4, furyl, thienyl, pyridyl, etc.)

The main method of synthesis of **1** and **2** is the aldol condensation of cyclic ketones with appropriate aldehydes in the presence of bases, Lewis acids and other miscellaneous catalysts[19]. It is well-known that aldol condensation is a stereoselective process and its products normally contain the double bond in the trans-configuration [20–22]. The same is true for bis(aryl-methylidene)cyclanones **2**, the most stable isomers of which are E,E-isomers, as depicted in the Scheme above. The lower stability of Z-isomers was explained by strong steric repulsion of aryl group and carbonyl oxygen[23].

Surprisingly, among hundreds studies of aryl- and heteroaryl derivatives the pyrrole analogs were undeservedly ignored: there are only two published papers [11, 24] mentioning enones **1** and **2**, (Ar = 2-pyrrolyl, n = 1,2). No structural information was given.

At the same time, these compounds containing the pyrrole motif are of special interest because possible formation of intramolecular hydrogen bond(s) can influence their structure and isomeric composition by stabilization of the Z-isomers (Scheme 1):

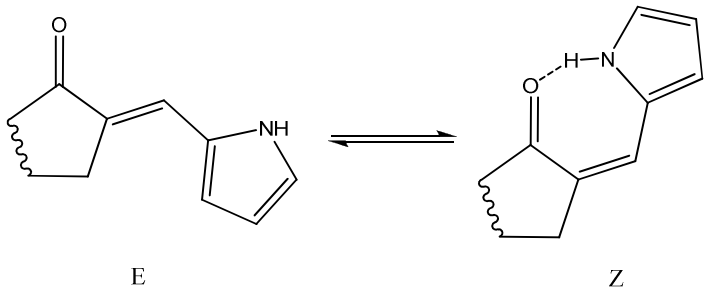

Scheme 1. E-Z isomerism of 2-pyrrolylidene-cycloalcanones.

Recently, we have studied the properties of similar hydrogen bonds in the 2-pyrrolylidene substituted 1,3-undandione and its derivatives [25]. Besides, we have found that these indandione derivatives can act as color sensors for fluoride and acetate anions, and that this ability is based on deprotonation of the pyrrole NH group [26].

Here we report on the synthesis of the series of compounds **3–7** and the study of their structure by X-ray (**3–5**), NMR and IR spectroscopy supported with DFT quantum chemical calculations.

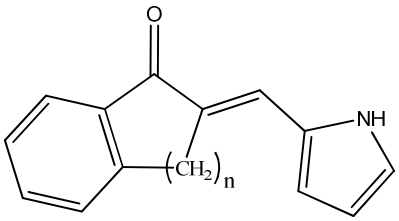

3 (n=1), 4 (n=2)

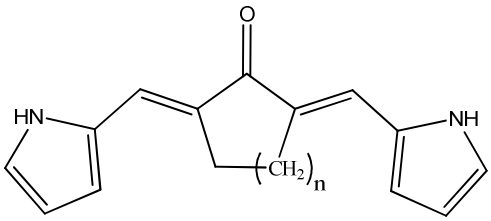

5 (n=1), 6 (n=2), 7 (n=3)

Results and Discussion

Synthesis

Synthesis of compounds **3–7** was carried out by condensation of 1*H*-pyrrole-2-carbaldehyde with corresponding cyclic ketones by heating at reflux in aqueous ethanol in the presence of potassium hydroxide, as shown below.

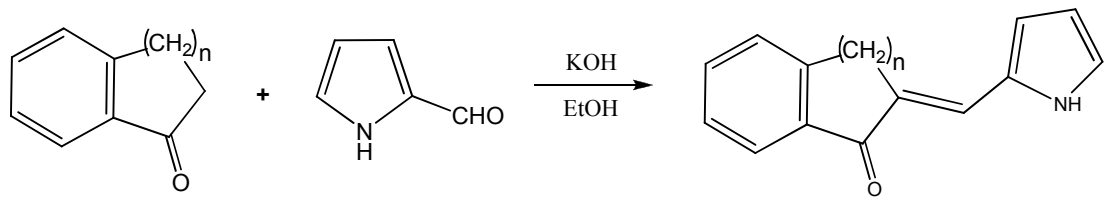

3 (n=1), **4** (n=2).

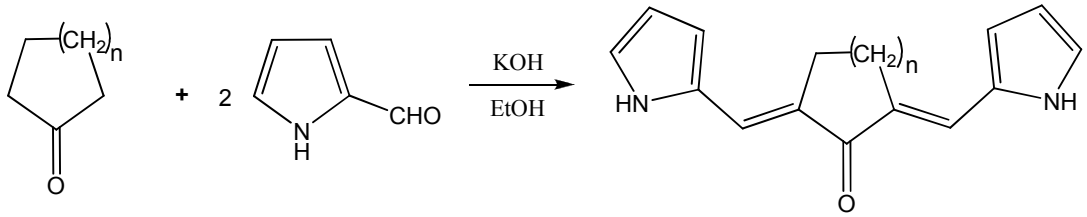

5 (n=1), **6** (n=2).

Scheme 2. Synthesis of studied compounds **3** - **6**

The reaction of cyclopentanone or cyclohexanone with two equivalents of the aldehyde during 3 h of heating results in the formation of a single product, the diadduct, whereas cycloheptanone reacts in more complex way and much more slowly. The conversion after 48 h reflux with 3-fold excess of 2-pyrrolylcarbaldehyde was 70% and 30% of the starting aldehyde was recovered. In the reaction mixture four compounds were identified: two monoadducts (*Z*)- and (*E*)-2-((1*H*-pyrrol-2-yl)methylene)cycloheptanones (**7a** and **7c**, respectively) and two diadducts (2*Z*,7*E*)- and (2*E*,7*E*)-2,7-bis((1*H*-pyrrol-2-yl)methylene)-cycloheptanones (**7b** and **7d**, respectively). Compounds **7a** and **7b** containing Z-moieties were isolated by column chromatography on silica gel using CH_2Cl_2 as an eluent. The mixture of **7c** and **7d** was not separated, but the structure of

its components was unequivocally proved and the ratio determined by ^{1}H and ^{13}C NMR spectroscopy (vide infra).

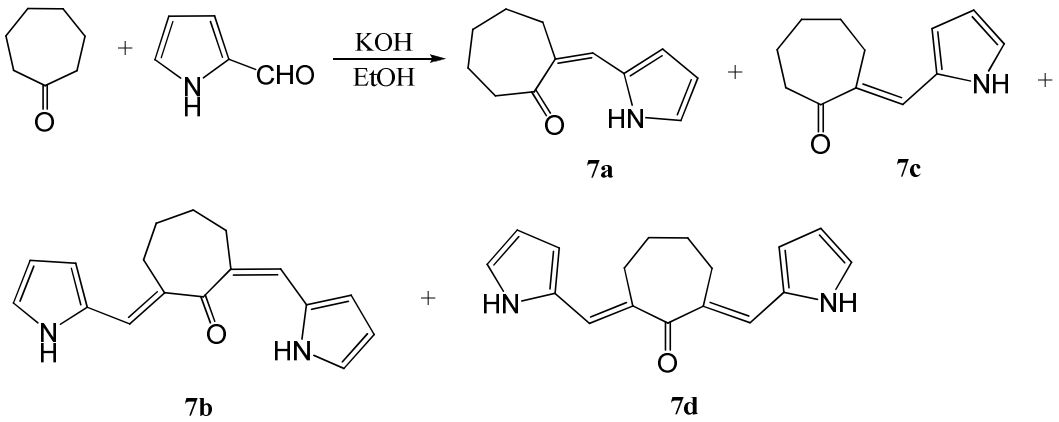

Scheme 3. Isolated products of reaction of cycloheptanones with 2-pyrrolylaldehyde

Compounds **3–6** are high-melting solids of yellow, orange or red color, obtained in a good yield (up to 93%).

X-ray analysis

The X-ray data of compound **3** confirm the E-configuration of the molecule (Fig. 1a). In the crystal, of C2h symmetry are formed with N-H···O=C hydrogen bonds of 2.0210(13) Å length (Fig. 1b). Molecule **3** is practically planar and the dimers are arranged in one plane. Note a reduced contact of ca. 2.8 Å between the *ortho*-hydrogen atom of the benzene ring of one molecule and the β-carbon atoms of the pyrrole ring of the other molecule of the dimer (Fig. 1c). The intersection angle between the planes of the molecules is ca. 54˚ (Fig. 1c) leading to the so-called 'parquet packing' (Fig. 1d).

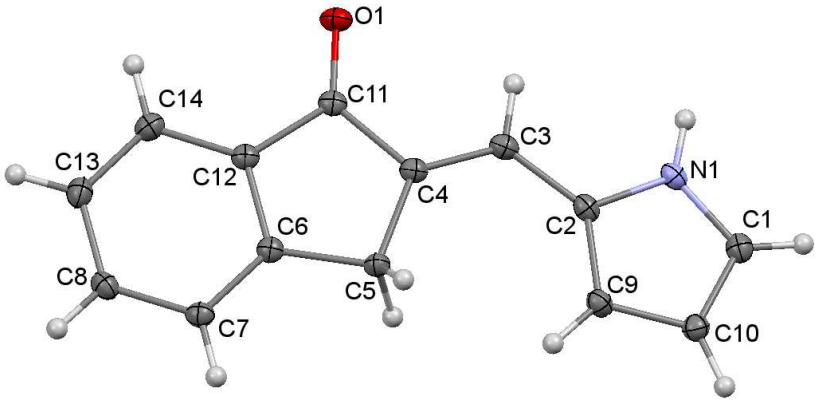
O1
C14
C11
C3
C13
C12
C4
N1
C6
C2
C1
C8
C5
C9
C7
C10

a

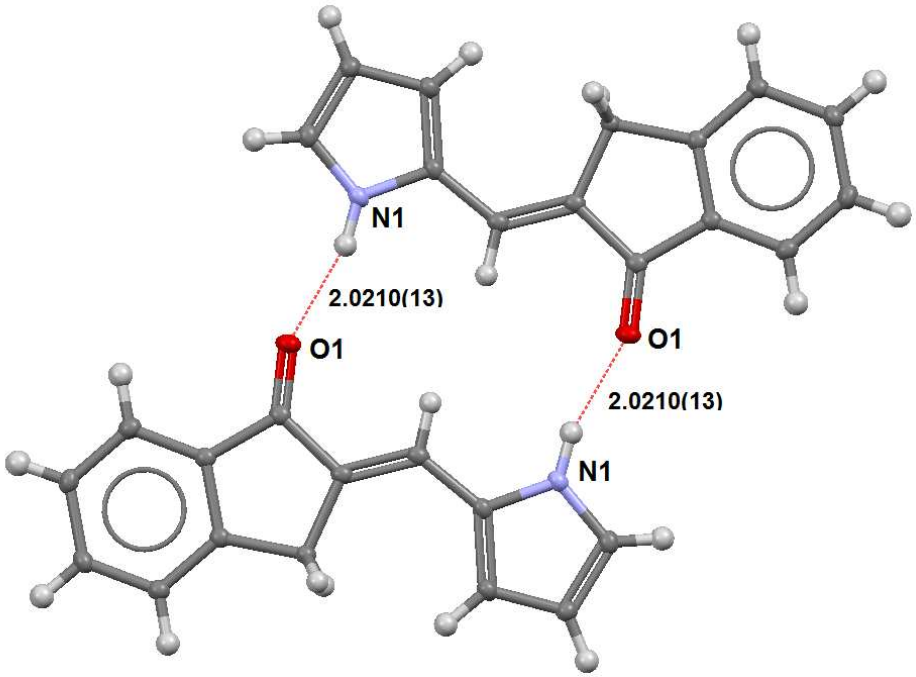
N1
2.0210(13)
O1
O1
2.0210(13)
N1

b

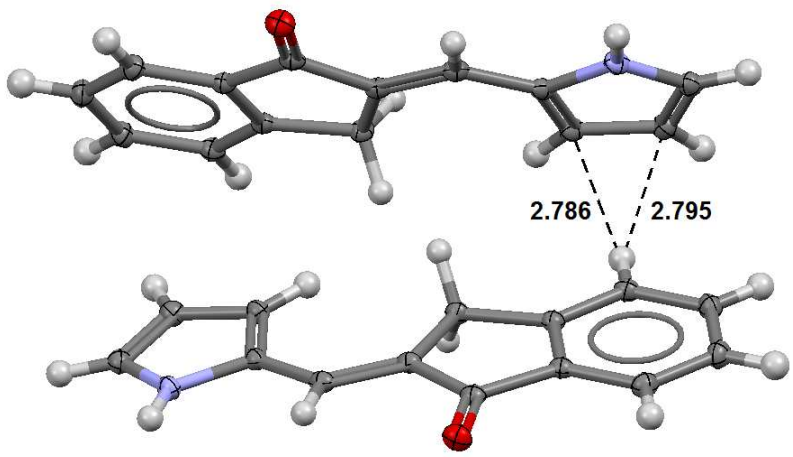

c

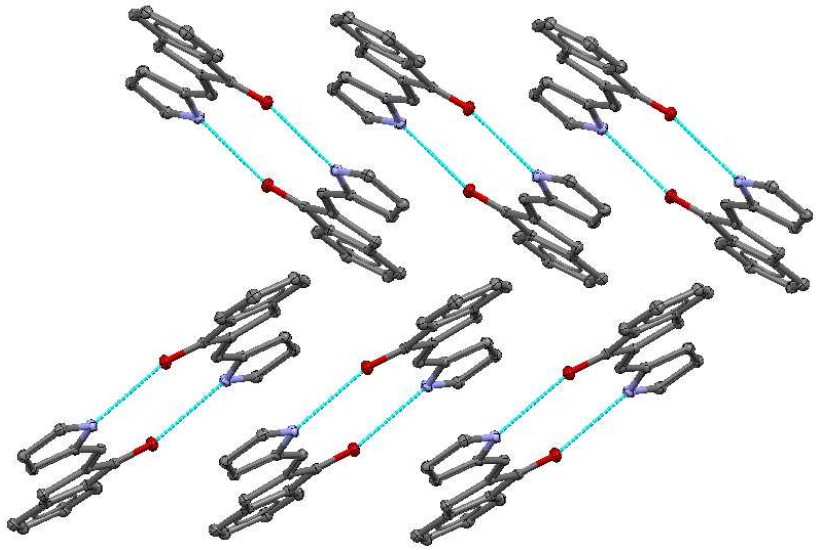

d

Figure 1. The molecular and crystal structure of compound **3**: molecular structure (a, ORTEP, 50% probability contours), the 'in-layer' H-bonded dimer structure (b), the 'between-layer' coordination (c), the 'parquet packing' in the crystal of **3** (d).

Similar to compound **3**, the molecules of compound **4** (Fig. 2a) form dimers in the crystal (Fig. 2b). Unlike in compound **3**, the molecules of **4** are not planar. The N–H···O=C intermolecular hydrogen bonds in **4** are 0.05 Å shorter than in **3**. The dimers form lamellar structure with the interlamellar distance of 2.691 Å (Fig. 2c). The layers are linked by weak interaction between one of the CH2 hydrogen atoms and the carbonyl oxygen of the second molecule.

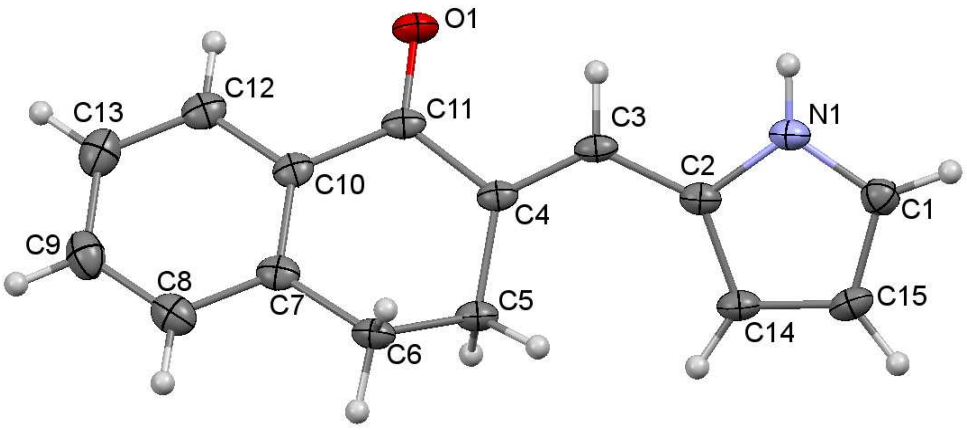

a

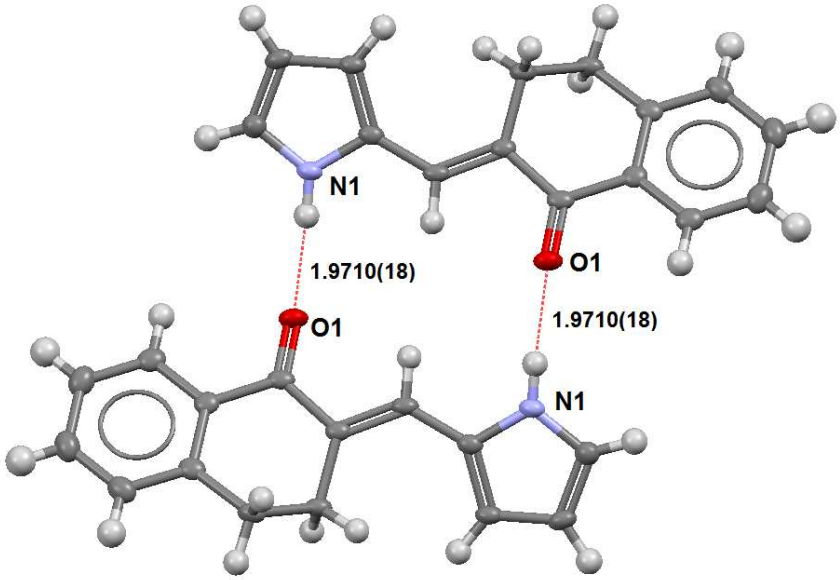

b

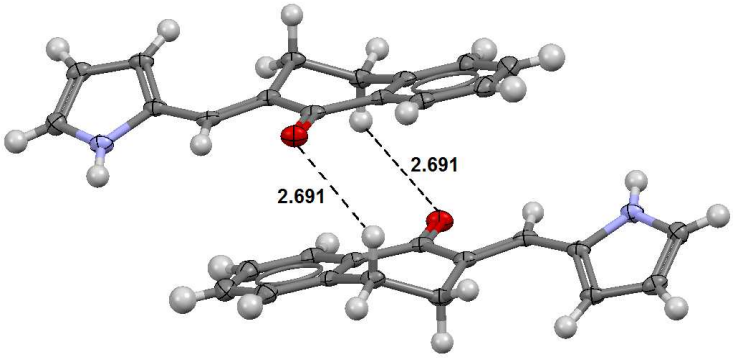

c

Figure 2. The molecular and crystal structure of compound **4**: molecular structure (a, ORTEP, 50% probability contours), the 'in-layer' H-bonded dimer structure (b), the 'between-layer' coordination (c).

According to X-ray data, the elementary cell of compound **6** contains two molecules with the E,E-configuration differing by orientation of the pyrrole rings to the rest of the molecule, the orientation being the same in the **6-E,E-cis,cis** conformation and the

opposite in the **6-E,E-cis,trans** conformation (Figure 3):

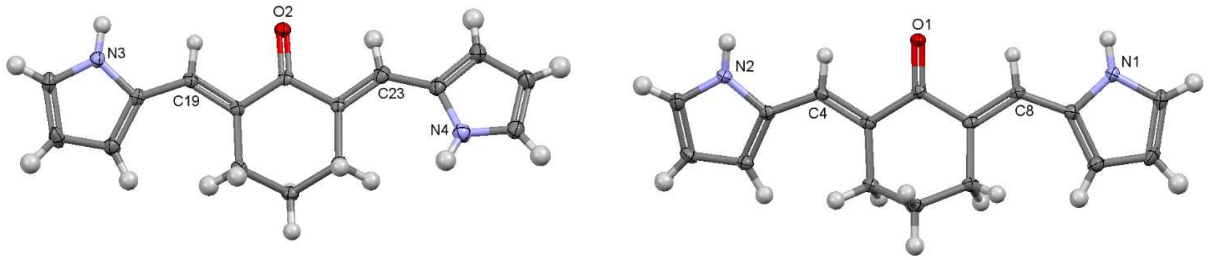

6-E,E-cis,cis **6-E,E-cis,trans**

Figure 3. Two conformations of **6-E,E** in the solid state

Asymmetric part of unit cell of compound **6** is shown in Fig. 4a. The structural motif of the crystals includes four molecules connected by hydrogen bonds (Fig. 4b). The oxygen atoms of the cis,cis-isomer form bifurcate hydrogen bonds with the NH groups of the cis,trans-isomer and another molecule of the cis,cis-isomer forming the tetramer depicted in Fig. 3b. The hydrogen bond lengths are: N1–H···O2=C 2.0060(19) Å, N2–H···O1=C 2.025(2) Å, N3–H···O1=C 2.0120(18) Å. Note, that the bifurcate bonds N2–H···O1=C and N3–H···O1=C are expectedly longer than the two-centered hydrogen bond N1–H···O2=C. Note also that the second NH group of the cis,trans-isomer is not involved in hydrogen bonding.

.

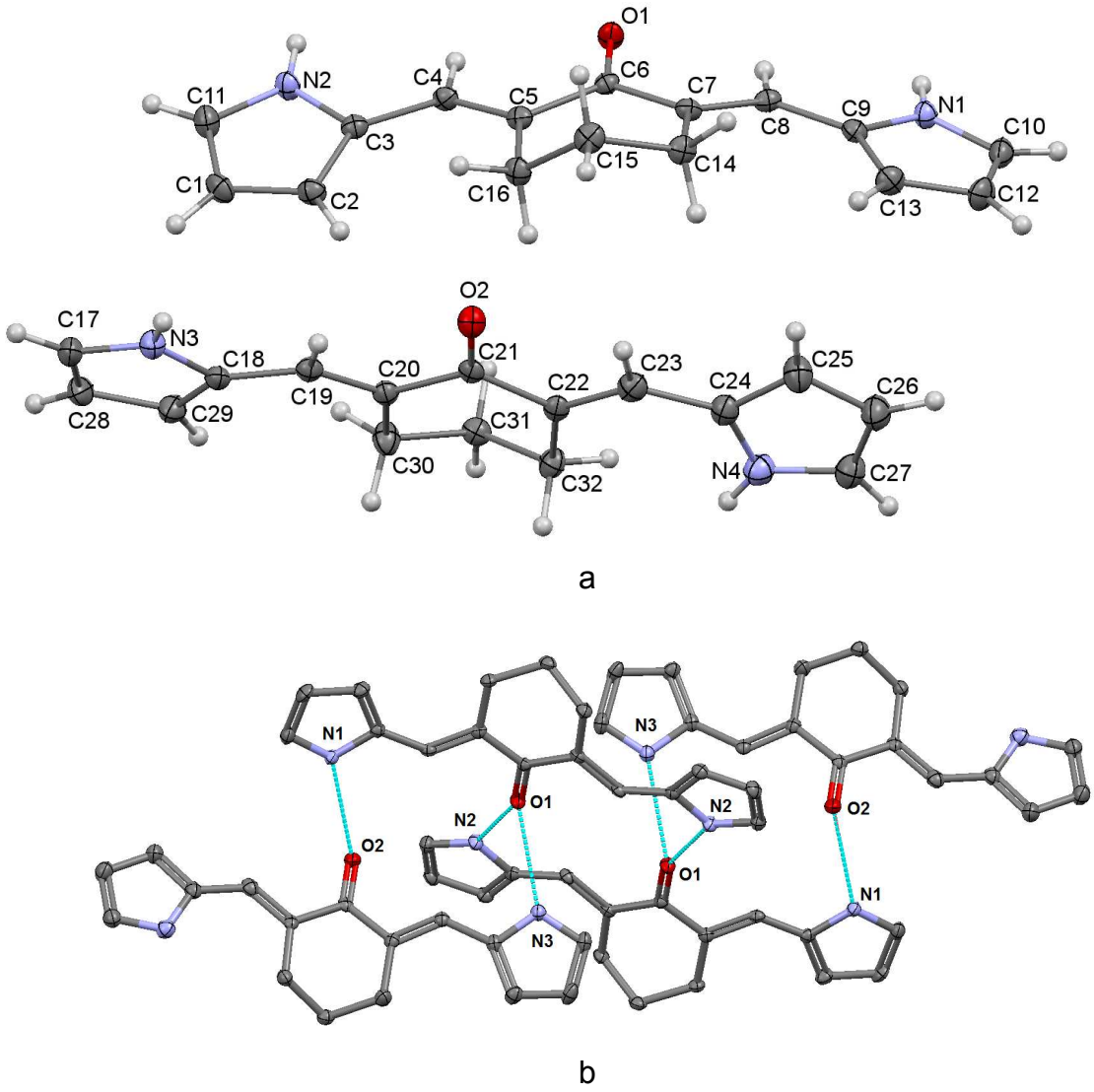

Figure 4. The molecular and crystal structure of compound **6**: asymmetric unit of molecular structure (a, ORTEP, 50% probability contours), the H-bonded tetramer structure (b).

NMR spectroscopy study

According to ^{1}H NMR spectra, the studied molecules retain their E-configuration on going from solid state to solution. The spectra of compounds **3–6** (Fig.S7-S10) contain the signal of the olefinic proton =CH at 7.3–7.9 ppm in $CDCl_3$ or DMSO-d_6 solution,

which, in full agreement with the earlier observations [19] is indicative of the anti-orientation of the 2-pyrrolyl substituent relative to the carbonyl group. The chemical shifts of the NH proton of all compounds in $CDCl_3$ solution lie in the range 8–9 ppm. In DMSO-d_6, due to formation of intermolecular hydrogen bond with solvent molecules, the NH signal is shifted to approximately 11 ppm.

Formation of hydrogen-bonded associates in solution, similar to the above-mentioned solid-state dimers, is also proved by ^{1}H NMR spectra. Consecutive dilution of the $CDCl_3$ solution of **3** (Fig. 5) results in a high-field shift of the NH and =CH signals by 0.50 and 0.11 ppm, respectively, whereas all the rest of the signals remain unchanged. These changes are a direct consequence of cleavage of the dimeric complex.

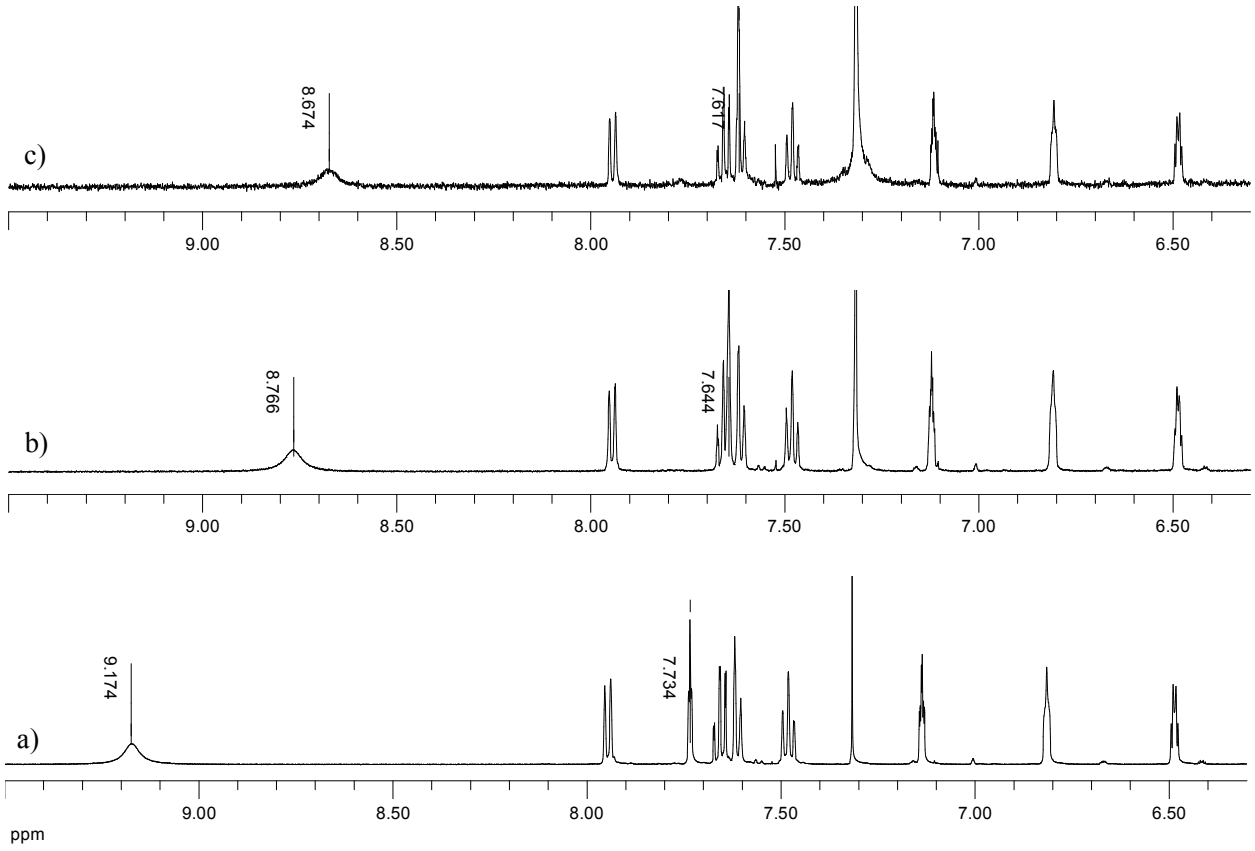

Figure 5. ^{1}H NMR spectra of **3** in $CDCl_3$. a) saturated solution; b) 3-fold dilution; c) 10-fold dilution.

The ^{1}H NMR spectra of both the E,E and Z,E-isomers of **6** in $CDCl_3$ show similar changes (see below), except that 10-fold dilution of the saturated solutions leads to only 0.06 - 0.08 ppm displacement of the NH signal (Fig. S15 and S16). Due to the lower solubility of **6** in $CDCl_3$, the concentration of the dimer is much less than in the case of **3**.

Photo-induced Z,E-isomerization and hydrogen bonding

The ability of chalcones and their cyclic analogs for photoisomerization and photodimerization is well-known in the literature [27-29].

UV irradiation of the solutions of the E-isomers of compounds **3**, **4** as well as of the E,E-isomers of compounds **5** and **6**, leads to isomerization around the double bonds with the formation of Z-isomers (for the first pair of compounds) and Z,E and Z,Z-isomers (for the second one) containing intramolecular NH···O=C hydrogen bonds (Scheme 4):

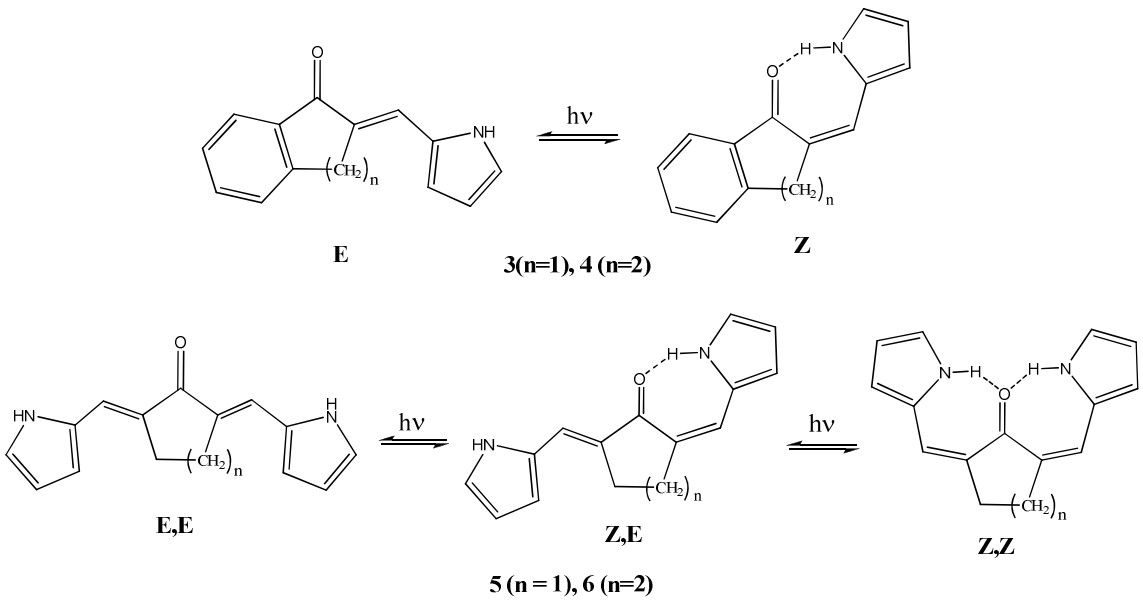

Scheme 4. The photo-isomerization products

The main characteristic feature of the Z-isomers of all studied compounds is a low-field signal of NH protons in the range 12–13 ppm, which is displaced downfield by 3–3.5 ppm relative to the signals in the E-isomers, thereby indicating the existence of a strong hydrogen bond N–H···O. On the other hand, the signal of the olefin proton in the Z-moiety, due to its remoteness from the carbonyl group, is displaced upfield by about 1 ppm.

As an example, the ^{1}H NMR spectrum of compound **3** after UV irradiation is given in Fig. S17.

The structure of the Z,E-isomers is proved by the appearance of two new signals of pyrrolic NH protons (see Fig. 6 for compound **5**) at 13.20 (intramolecularly hydrogen bonded) and 11.56 ppm (intermolecularly H-bonded with the solvent molecule); besides, two sets of signals are observed belonging to the E-part and Z-part of the molecule: six signals of the pyrrole rings and two signals of olefinic protons at 7.40 (E-part) and 6.82 ppm (Z-part).

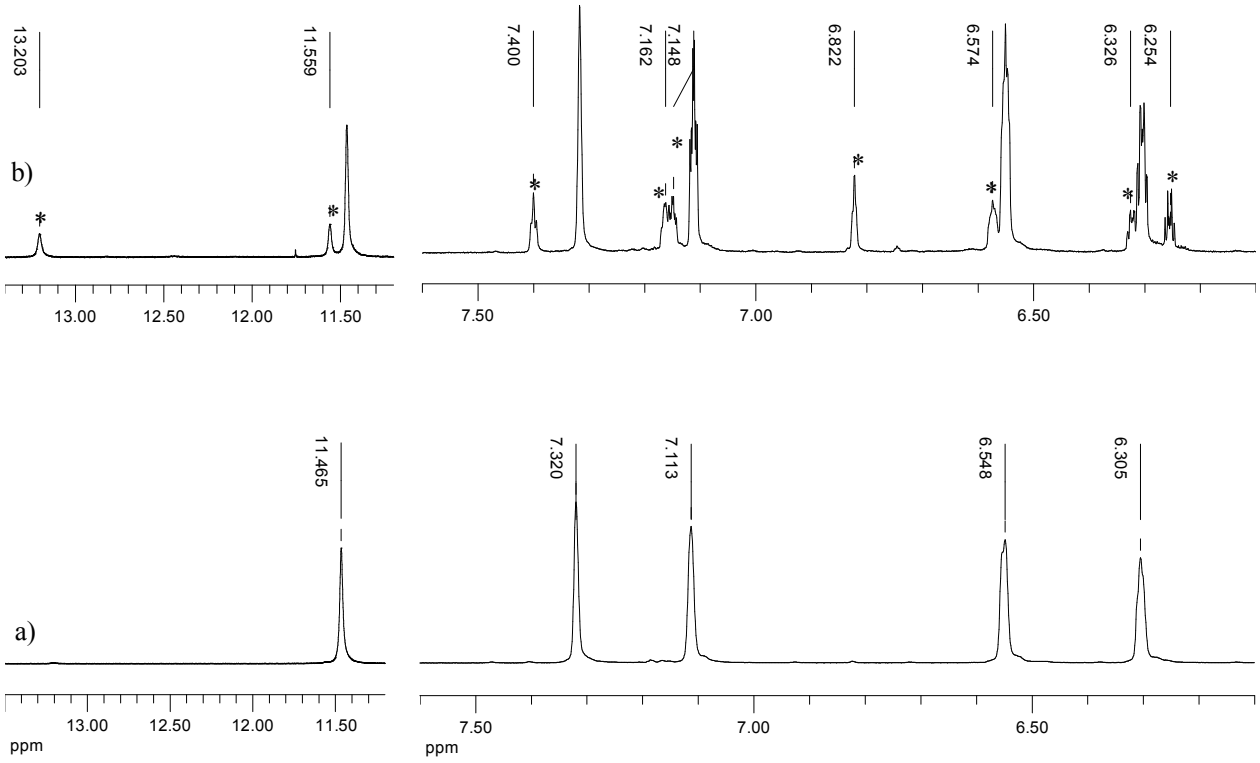

Figure 6. ^{1}H NMR spectra of **5** in DMSO-d6: a) without irradiation; b) after 3.5 hours of UV irradiation at 365 nm. Non-overlapping signals of **5-Z,E** isomer are marked by asterisks.

Formation of the Z,Z-isomer upon UV irradiation was observed for the cyclohexanone derivative **6**. Fig. 7 shows the ^{1}H NMR spectrum of **6** in CD_3CN after 3.5 h exposure at 365 nm wavelength. The mixture consists of **6-E,Z** isomer as the predominant compound (about 90%) and 10% of the minor **6-Z,Z** isomer. The **6-E,E** isomer is not observed. In another experiment, the isolated **6-E,Z** isomer was irradiated in CD_2Cl_2 solution for 2 h; the resulted mixture consisted of ca. 75% of **6-E,Z** and 25% of **6-Z,Z** isomers, but the concentration of the latter compound was significantly diminished (to 10%) after standing overnight.

The low content of the **6-Z,Z** isomer and its relatively quick reconversion is indicative of its lower stability with respect to the **6-Z,E** isomer, in spite of expected stabilization by the two intramolecular hydrogen bonds.

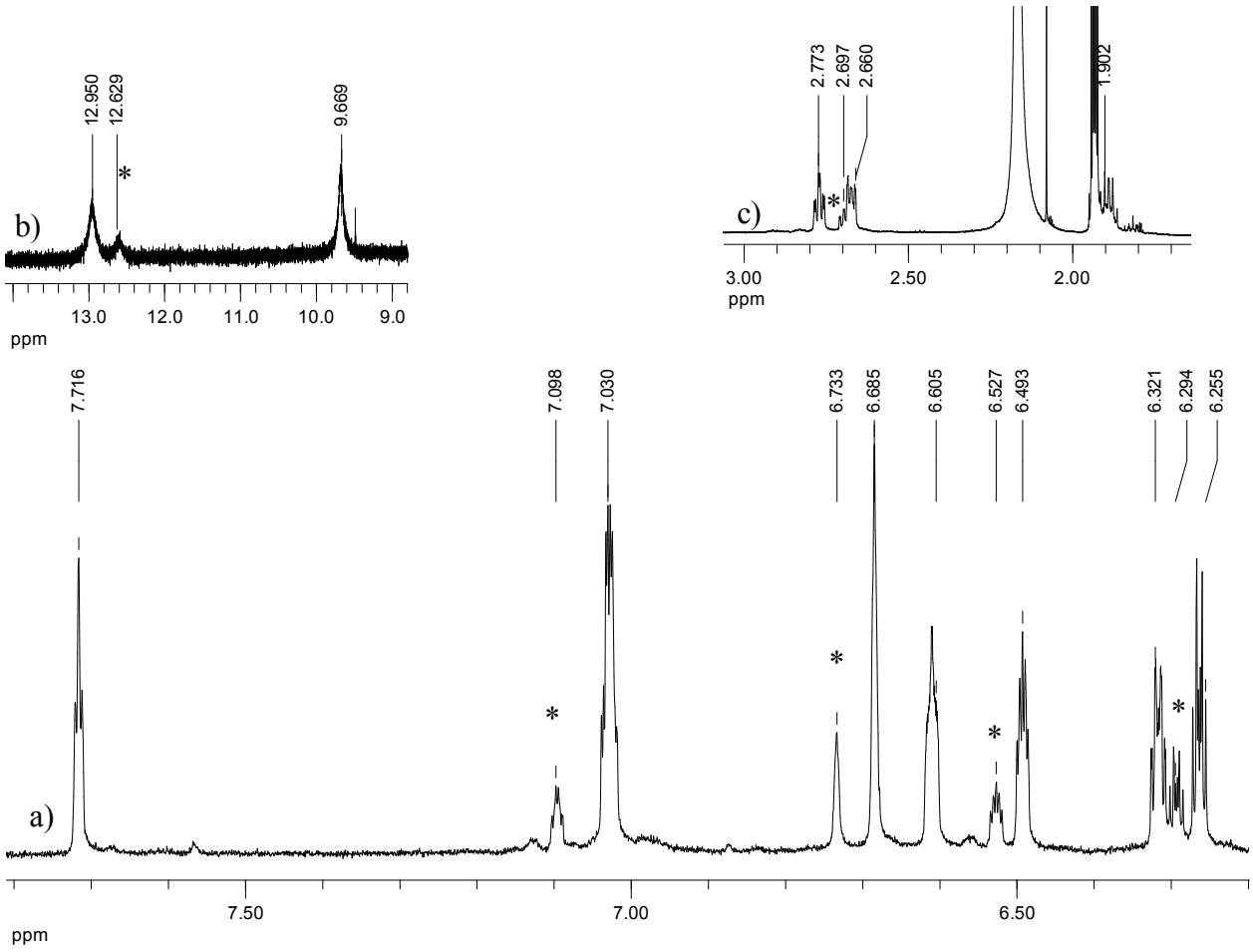

Figure 7. ^{1}H NMR spectrum of **6** in CD_3CN irradiated at 365 nm for 3.5 hours: a) aromatic region; b) NH region, c) alkyl region. The signals of **6-Z,Z** are marked by asterisks.

The isomerization process is strongly dependent on the nature of the compound and solvent (Table 1). Thus, irradiation of the solution of **5** in DMSO-d_6 during 6 hours results

in conversion of only 9% of the **5-E,E** isomer to **5-Z,E**, whereas compound **6** under the same conditions gives about 20% of **6-Z,E** isomer. Similarly, compound **3** in DMSO isomerizes only partially (40% during 45 min of irradiation), whereas in acetonitrile during the same exposition time the amount of isomerized compound is two times larger (76%). For compound **6** in acetonitrile solution, isomerization is also fast: it almost completely isomerizes after 2 hours of irradiation, and besides Z,E-isomer (predominant) some amount of Z,Z-isomer is also formed. On the other hand, the reverse transformation from Z- to E-isomers in acetonitrile solution is very slow (Table 1, Fig. S9); it is worth to mention that the concentration of **6-Z,E** remains almost constant during 10 days. Apparently, this is indicative of the two-step isomerization, Z,Z → Z,E and Z,E → E,E, when the loss of concentration of the intermediate **6-Z,E** isomer in the second step is compensated by its accumulation in the first step.

Table 1. Interconversion of isomers of **3, 5,** and **6** subjected to UV-irradiation[a)].

Time after irradiation	**3**, CD3CN, 45 min[b)]	**3**, DMSO-d6, 45 min [b)]	**5**, DMSO-d_6, 6 h[b)]	**6**, DMSO-d_6, 6 h [b)]	**6**, CD_3CN, 2 h[c)]
0	0.76	0.40	0.09	0.20	0.82/0.013/0.16
24 hours	0.51	0.33	0.07	0.15	0.83/0.022/0.14
48 hours	0.43	0.29	0.05	0.12	0.84/0.025/0.13
72 hours			0.05	0.08	0.84/0.04/0.11

96 hours	0.38	0.27	0.05	0.06	0.83/0.07/0.10
240 hours					0.82/0.1/0.08

[a] Substrate, solvent, and exposition time are indicated.

[b] Numbers represent the fraction of Z-isomer (for **3**) or Z,E-isomer (for **5** and **6**).

[c] Numbers represent the fractions of Z,E-, E,E – and Z,Z-isomer respectively (for **6**).

The drastic solvent influence on the E-Z-isomerization rates may have following reasons. It is known that E-Z photoisomerization of trans-stilbenes is slowing down on going from non-polar solvents to polar ones [30]. Besides, weakening of hydrogen bonds in the excited states is a well-documented phenomenon [31]. In the case of studied compounds **3**–**7** the hydrogen-bonded dimers break down under UV irradiation and the monomer molecules are expected to isomerize more easily to more stable Z-isomers (see below). The two effects may also act synergistically.

The chemical shifts of hydrogen-bonded NH deserve a special attention because they are directly related to the strength of the hydrogen bond. The corresponding values of NH chemical shifts are collated in Table 2.

Table 2. NH proton chemical shifts for Z, E-isomers of **5**-**7**

	CD_2Cl_2		DMSO-d_6	
Entry	δ (NH…O) intramol.	δ (NH) free	δ (NH…O) intramol.	δ (NH) free
5-Z,E	13.08	8.72	13.20	11.56
6-Z,E	13.02	8.97	12.80	11.49
7-Z,E	11.80	8.66	11.34*	11.34*

*Overlapping signal with integral intensity of 2H

From the comparison of the chemical shifts it unambiguously follows that hydrogen bonds in compounds **5** and **6** are of equal strength and significantly exceed that in compound **7** (corresponding chemical shift difference values are of 1.28 and 1.22 ppm). For compounds **6** and **7**, dissolution in DMSO-d6 results in that the initially weaker hydrogen bond in cycloheptanone derivative 7 suffers a stronger weakening by the action of DMSO than in **5** and **6**. These findings will be discussed below in connection with theoretical calculations.

Interaction with fluoride and acetate anions

In this section the behavior of the E,E and Z,E-isomers of compound **6** in the presence of tetrabutylammonium fluoride (TBAF) and acetate (TBAA) is described. Recently [26], we have shown that 2-pyrrolylidene derivatives of 1,3-indandione in the presence of these salts undergo NH-deprotonation, which is accompanied by the change of the

solution color from yellow to orange and by drastic changes in the ^{1}H NMR spectra indicating that the intramolecular hydrogen bond N–H···O in the neutral molecule is replaced by the C–H···O hydrogen bond in the anion.

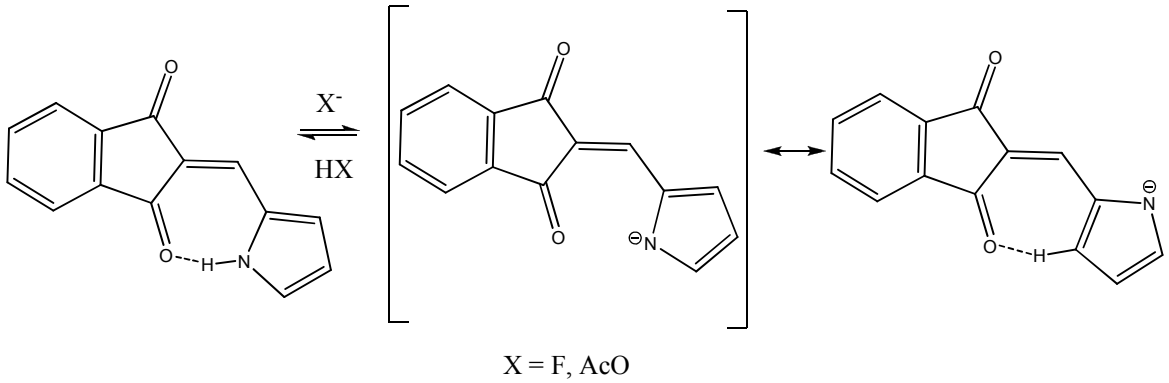

Scheme 5. Interaction of 2-pyrrolylidene-1,3-indandione with acetate and fluoride anions

This finding allowed us to consider these indandione derivatives as potential sensors of fluoride and acetate anions [26]. Based on close structural similarity of these compounds and **2–6** one can expect the manifestation of anion sensor properties also for the last series.

However, the addition of TBAA to DMSO-d_6 solution of **6-E,E** revealed neither color variations, nor noticeable changes in the ^{1}H NMR spectrum, except for a downfield shift of the NH signal from 11.5 to 13.5 ppm, indicating the formation of a hydrogen bond with acetate ion.

In a similar manner behaves the **6-Z,E** isomer, which also does not change its color upon addition of TBAA and shows almost the same variations in the ^{1}H NMR spectrum (a downfield shift of the free NH proton by 2.2 ppm. At the same time, the signal of

intramolecular hydrogen bonded NH proton of the Z-moiety remains almost unchanged (Fig. 8).

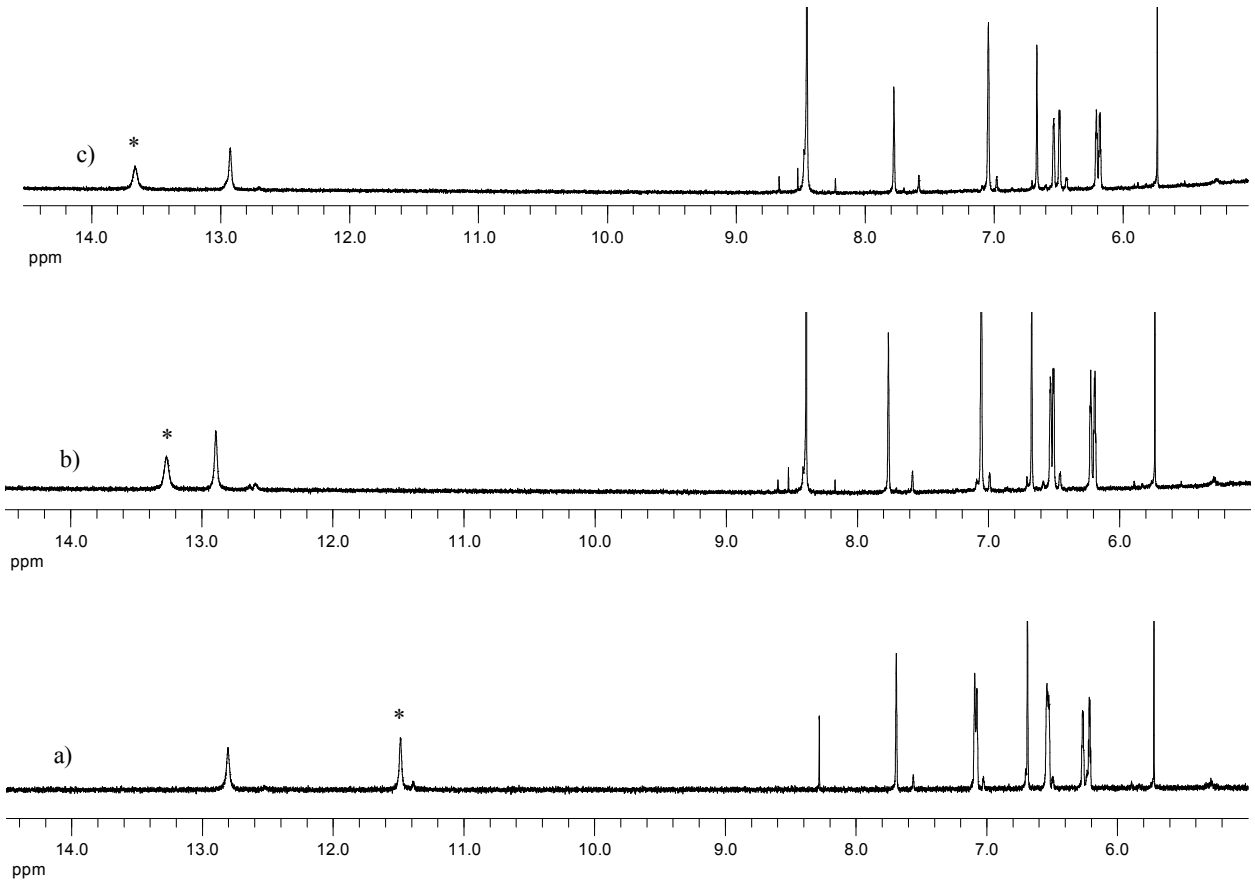

Figure 8. ^{1}H NMR spectra of **6-Z,E** in DMSO-d_6: without (a)) and with consecutive additions (b) and c)) of tetrabutylammonium acetate. The NH signal of E-moiety is marked by asterisks.

In contrast, addition of TBAF to the solution of **6-E,E** in DMSO-d_6 changes the color of the solution from yellow to dark-red. Addition of TBAF has a slight effect on the ^{1}H NMR signals of aromatic and olefinic protons, but causes disappearance of the NH signal at 11.45 ppm and appearance of a characteristic triplet of HF_2^- at 16.1 ppm (J = 122 Hz)

indicating the deprotonation of one of the pyrrole rings (Fig. S19). The other NH proton is not observed, most probably because of fast exchange.

The similar color changes occur upon TBAF addition to DMSO-d_6 solution of **6-Z,E**, but the ^{1}H NMR spectrum of **6-Z,E** in the presence of TBAF, apart from the appearing of the HF_2^- triplet at 16.1 ppm, is quite different (Fig. 9):

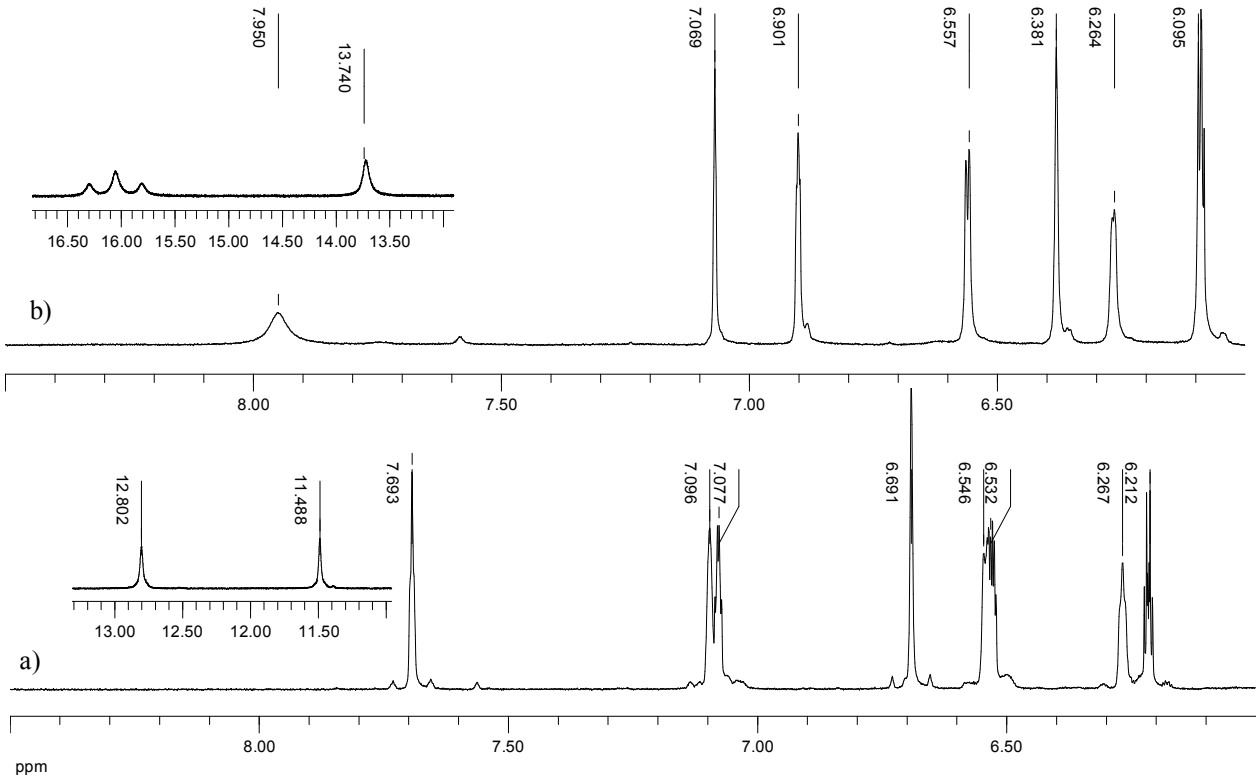

Figure 9. Aromatic and NH regions of ^{1}H NMR spectra of **6-Z,E** in DMSO-d_6 (a) and with excess of Bu_4NF (b).

The NH signal at 11.49 belonging to the E-moiety (hydrogen bonded with the solvent) disappears whereas the signal of the intermolecularly bonded NH moves downfield to

13.74 ppm which being compared with its chemical shift of 12.80 ppm in the neutral molecule indicates the strengthening of the hydrogen bond in the anion:

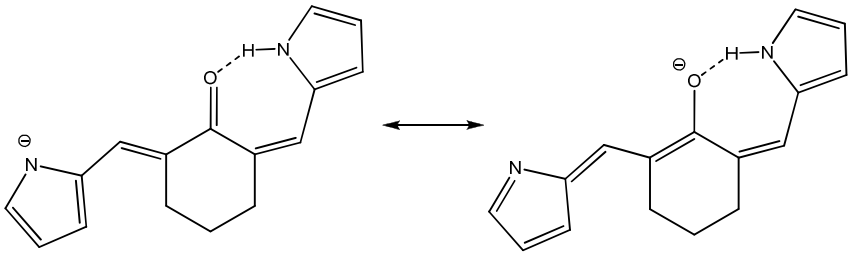

Scheme 6. Strengthening hydrogen bond N-H…O by anion formation

The signals of the olefinic protons of the E and Z-moieties are shifted by 0.25 to low field and by 0.3 ppm to high field respectively, the former one being broadened; the shifts of other protons are less affected (Fig. 9).

Due to the difference in behavior of the studied compounds with respect to acetate and fluoride anions (sharp color change in the last case) one can suppose that these compounds possess a higher selectivity towards the fluoride ion than the earlier described 1,3-indandione derivatives [26].

IR spectroscopic study

In the IR spectra of compounds **3** and **4** in the solid state the intermolecular hydrogen bonds NH···O=C are characterized by the νNH bands at 3269 and 3278 cm^{-1} and the νC=O bands at 1674 (Figure 10) and 1651 cm^{-1}, respectively. In CCl_4 solution, these bonds are partly dissociated and the spectrum contains both the above associated bands and the bands of free C=O groups of **3** and **4** at 1697 and 1666 cm^{-1}, respectively. The doublet bands of vibrations of the free NH groups at 3496 and 3471

cm^{-1} suggest the presence in the solution of two conformers of the E-isomer with the opposite orientation of the pyrrole ring. Complete dissociation of the NH···O=C hydrogen bond occurs in solutions of **3** and **4** in CH_2Cl_2. The IR spectra of both compounds contain doublet bands of free NH groups at 3490 and 3450 cm^{-1} each, and free C=O groups at 1689 (**3**) and 1660 cm^{-1} (**4**).

In the IR spectrum of the irradiated compound **3** in CH_2Cl_2 (Figure 10), along with the bands belonging to the starting E-isomer, an intense band at 1665 cm^{-1} is observed. Its frequency is lower than that of the band of associated C=O groups appearing at 1674 cm^{-1} in the spectrum of solid compound. Appearance of this low-frequency ν(C=O) band is related with the formation of the Z-isomer of compound **3** with the intramolecular NH···O=C bond belonging to the category of strong resonance-assisted hydrogen bonds [32,33]. This explains the absence of the corresponding ν(NH) band in IR spectrum.

The IR spectrum of compound **5** in the solid state contains two low-frequency νNH bands: an intense band at 3264 cm^{-1} and a weak band at 3377 cm^{-1}. They correspond, respectively, to vibrations of NH groups forming a two-center hydrogen bond NH···O=C and a less strong bifurcate (NH)2···O=C intermolecular hydrogen bond. The band of vibrations of associated C=O groups appears at 1670 cm^{-1}. In the spectrum of a diluted solution of **5** in CH_2Cl_2 only the bands of free NH groups of the two conformational isomers are observed at 3480 and 3450 cm^{-1} and the band of the free C=O group at 1704 cm^{-1}.

Most strong intermolecular hydrogen bonds NH···O=C are formed in compound **6**. As a result, the ν(C=O) frequency in the IR spectrum of solid **6** is drastically decreased, so that the ν(C=O) and ν(C=C) vibrations become mixed and are characterized by a

common doublet band with maxima at 1589 and 1574 cm^{-1}(Figure 10). In the ν(NH) vibration range, weak bands at 3498 and 3471 cm^{-1} are observed, in agreement with the presence of free NH groups in the conformers of E,E isomer of **6** differing by the N–$C_{2'}$–C_{α}–H angle (0 or 180º). Besides, a wide band is observed, with poorly resolved maxima at 3254 and 3215 cm^{-1}, belonging to vibrations of the associated NH groups. The spectrum of a dilute solution of **6** in CH_2Cl_2 contains a single intense band at 1599 cm^{-1}, apparently belonging to mixed vibrations ν(C=O) and ν(C=C). This may be indicative of retention of the intermolecular NH···O=C hydrogen bonds in the dimer even upon dilution in CH_2Cl_2.

After UV irradiation in acetonitrile solution, the free C=O group band in the IR spectrum of compound **6** in CH_2Cl_2 appears at 1702 cm^{-1} (Figure 10). According to the NMR data (vide supra), irradiation results in the formation of the Z,E isomer. A low intense band at 1645 cm^{-1} in the spectrum is caused by the presence of a small amount of the conformer with intramolecular hydrogen bond NH···O=C in the solution. Note, that in CCl_4 solution of **6** the low frequency ν(C=O) band becomes more intense than the band of the free C=O group.

The IR spectrum of compound **5** in the solid state contains two low-frequency νNH bands: an intense band at 3264 cm^{-1} and a weak band at 3377 cm^{-1}. They correspond, respectively, to vibrations of NH groups forming a two-center hydrogen bond NH···O=C and a less strong bifurcate (NH)2···O=C intermolecular hydrogen bond similar to that in compound **6**. The band of vibrations of associated C=O groups appears at 1670 cm^{-1}. In the spectrum of a diluted solution of **5** in CH_2Cl_2 only the bands of free NH groups of the

two conformational isomers are observed at 3480 and 3450 cm^{-1} and the band of the free C=O group at 1704 cm^{-1}.

The IR spectrum of the CCl_4 solution of compound **7**, which is formed as a mixture of the hydrogen-bonded and nonbonded conformers of the Z,E isomer directly from the synthesis, without UV irradiation, contains two ν(C=O) bands – a weak one at 1703 cm^{-1} belonging to the nonbonded conformer and a more intense at 1644 cm^{-1} belonging to the intramolecularly H-bonded conformer.

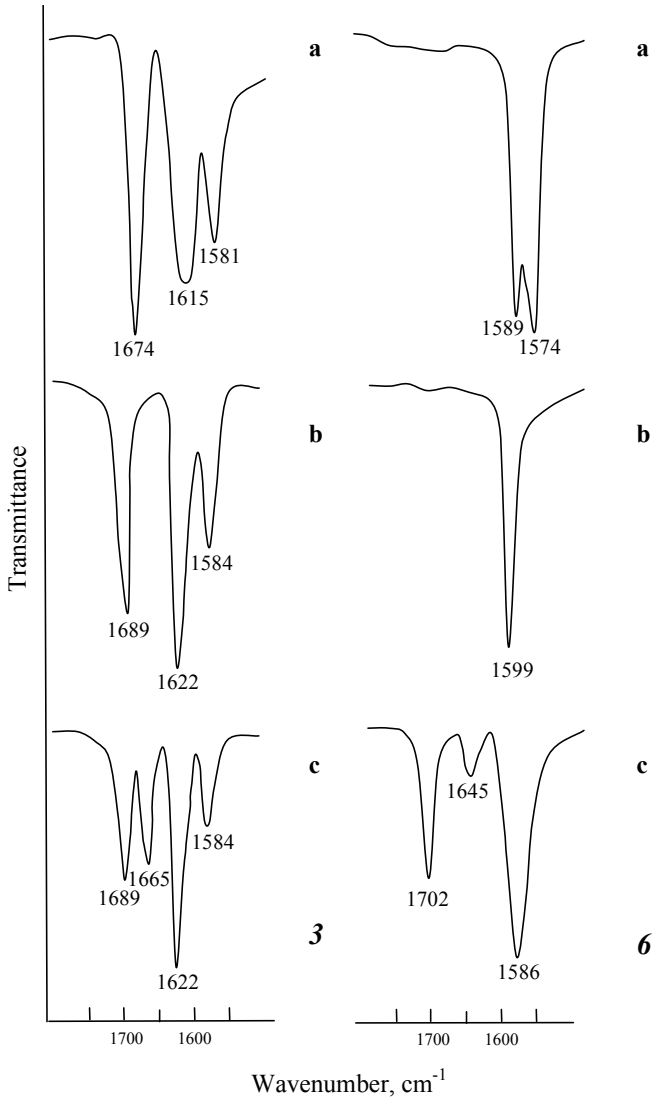

Figure 10. IR spectra of compounds **3**, **6** in the region 1800–1500 cm^{-1}: **a** – solid compounds in KBr, **b** – solutions in CH_2Cl_2, **c –** solutions in CH_2Cl_2 after UV irradiation.

Protonation

The molecules of the studied compounds contain several potential sites of protonation – the carbonyl oxygen and the pyrrole ring carbons C-3 and C-5. These sites have different basicity and nucleophilicity: carbonyl oxygen is very weak base and can be protonated only with strong acids like 96% sulfuric acid [34] or super acids [35]. On the other hand, the pyrrole ring due to its rather high basicity undergoes protonation even with relatively weak acids, for example trifluoroacetic (TFA) or HCl in non-aqueous media [36, 37]. For the studied compounds, the site of protonation can be easily determined by ^{1}H NMR spectroscopy because the spectral patterns in the case of the pyrrolium cation formation and protonation of the carbonyl oxygen should be quite different.

Upon addition of excess TFA to the solution of **6**-**E,E** in CD_3CN the bright yellow color turns deep-blue. In the ^{1}H NMR spectrum the number of signals and their multiplicity does not change but all of them are shifted to low field. Similar changes are observed in the ^{13}C NMR spectrum: both pyrrolic and olefinic carbon signals are shifted to low field by 4–10 ppm, except the carbonyl carbon which shows a high-field shift (Table 3). This fact unambiguously indicates that protonation of compound **6** occurs at the carbonyl oxygen atom. Addition of TFA to the solution of the isolated **6-Z,E**-isomer also changes the color to dark-blue and simultaneously the compound is completely isomerized to **6-E,E**. In the IR spectrum, the addition of TFA results in a gradual decrease (down to

vanishing) of the ν(C=O) band at 1599 cm^{-1} and appearance of a very strong band of protonated carbonyl group at 1553 cm^{-1}.

Interaction of the monosubstituted analog of **6**, compound **4**, with TFA is visually different from the previous one. The color of the acetonitrile solution changes from yellow to orange-red, and the variations of the chemical shifts are smaller (Table 3). Compound **4** also undergoes the Z⇆E isomerization, the ratio (Z/E) being 1:6. Interestingly, this ratio remains the same when TFA is added to the preliminarily irradiated sample of **4** in CD_3CN, in which the Z-isomer predominates. The observed low-field shift of the ^1H and ^{13}C signals of the pyrrolylmethyl moiety is notably less in **4** as compared to **6** (Table 3). It may be due to the fact that the incipient positive charge appears on the benzylic (with respect to the phenyl group) carbon atom in **4** and, therefore, is mainly stabilized by direct conjugation with the aromatic system. In **6**, all stabilization comes from donation from the two pyrrolyl groups, which results in larger low-field shift of the corresponding signals.

Table 3. Effect of protonation on ^1H and ^{13}C NMR chemical shifts of compounds **4** and **6**

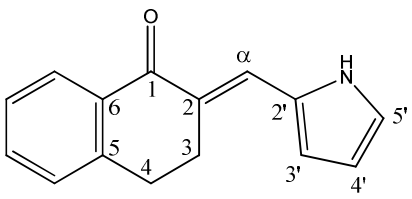

4

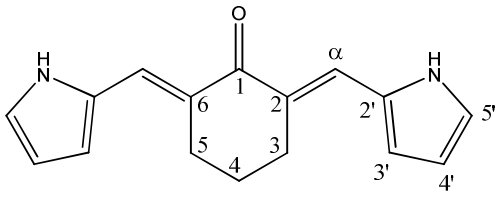

6

	4	**6**

Atom	^{1}H or ^{13}C chemical shift, δ*		$\Delta\delta$*	^{1}H or ^{13}C chemical shift, δ		$\Delta\delta$
	CD_3CN	CD_3CN + TFA		CD_3CN	CD_3CN + TFA	
NH	9.74 (12.77)	10.08 (12.77)	0.34 (0)	9.61	10.30	0.69
H-α	7.77 (6.96)	8.03 (6.99)	0.26 (0.03)	7.57	8.04	0.47
H-3'	6.72 (6.64)	6.94 (6.64)	0.22 (0)	6.56	7.14	0.58
H-4'	6.37 (6.36)	6.47 (6.35)	0.10 (-0.01)	6.29	6.56	0.27
H-5'	7.07 (7.14)	7.25 (7.14)	0.18 (0)	6.99	7.45	0.46
C-1				187.7	180.9	-6.8
C-2						
C-α	126.00	128.38	2.38	125.27	135.83	10.56
C-2'						
C-3'	113.77	115.48	1.71	113.72	123.42	9.70
C-4'	110.74	111.60	0.86	110.71	115.07	4.36
C-5'	122.16	124.00	1.84	121.93	131.58	9.65

*The numbers in parentheses correspond to ^{1}H chemical shifts and their differences (Δδ) for protonated **4-Z**-isomer.

Protonation of the carbonyl group in compounds **4** and **6** results in the formation of cations $\mathbf{4}^+$ and $\mathbf{6}^+$ with extended conjugated system.

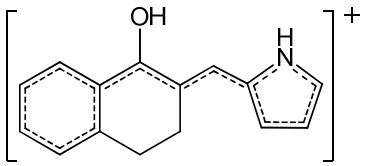

4^+

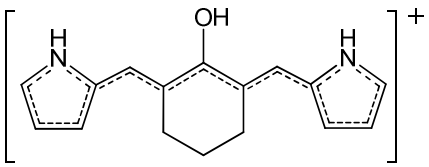

6^+

The extension of the conjugated system is expected to lead to changes in the UV-vis absorption spectra, in particular, to the appearance of a new longwave absorption band. Indeed, after addition of TFA, in the UV spectrum of the formed blue acetonitrile solution of **6** a longwave band appears, with the maximum at 594 nm. Its intensity increases with the increase of the acid concentration (Fig. 11). Simultaneously, the intensity of absorption bands with the maxima at 248 and 408 nm, caused by the $\pi\rightarrow\pi^*$ electron transitions in the conjugated system of the nonprotonated **6-E,E** isomer, is decreased. As distinct of that, the band appears and rises in intensity with the maximum at 218 nm, belonging to the $\pi\rightarrow\pi^*$ electron transitions of the alkyl substituted pyrrole ring [38]. Similarly, the addition of TFA to the solution of compound **4** in acetonitrile causes a decrease of intensity of the bands of $\pi\rightarrow\pi^*$ electron transitions with the maxima at 262 and 379 nm and growth of the band at 220 nm (Fig.11). The absorption band with the maximum at 379 nm suffers bathochromic (red) shift by 14 nm. The orange-red color of the solution is produced by the doublet longwave absorption band with the maximum at 514 nm and the shoulder at 488 nm. With addition of the acid, up to 1/3 of the total volume, the intensity of this band is increased. The fact that the new band in $\mathbf{4^+}$ appears at lower wavelengths than that in $\mathbf{6^+}$ is consistent with a more extended π-conjugated system in the latter cation.

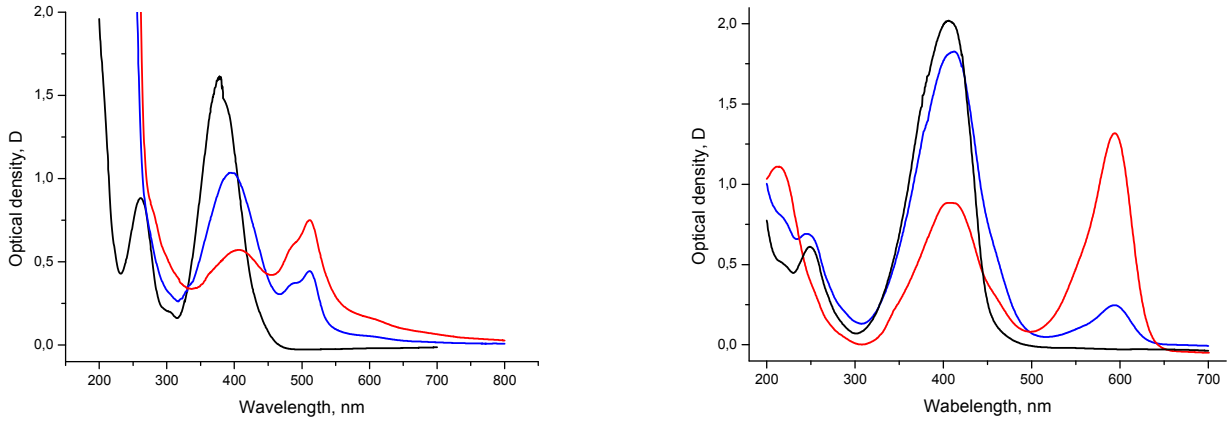

Figure 11. UV-vis spectra of cations **4**$^{+}$ (left) and **6**$^{+}$ (right) in acetonitrile without TFA (black), with one drop of TFA (blue) and two drops of TFA added (red).

Theoretical calculations

First, the energies of all possible isomers at the exocyclic double bond of compounds **5–7** were calculated on the optimized geometries at the level of B3LYP/6-311G(d,p). Expectedly, the stability of the isolated molecules increases in the order *E,E* < *E,Z* < *Z,Z* being determined by the presence and number of intramolecular hydrogen bonds, Table 3. However, the experimental data described above both in the solid state and solution show that the products formed in the condensation reaction have the *E,E*-configuration, and are photoisomerized to the E,Z- and *Z,Z*-isomers (at least, for the five- and six-membered ring substrates) only by UV irradiation. How can this apparent contradiction between the experimental and theoretical results be reconciled? Most probably, assuming that in a condensed polar medium the relative stability of possible associates of specific isomers rather than that of the isolated molecules should be considered,

especially if they contain strong basic and acidic centers in the molecule, as is the case for compounds **3–7**. To check this assumption we have calculated total energies of the cyclic dimers formed from the *E,E* and *E,Z*-monomers by closing the ring by two hydrogen bonds, considering them as models of self-associates existing in solution, as depicted below (Table 4, 5):

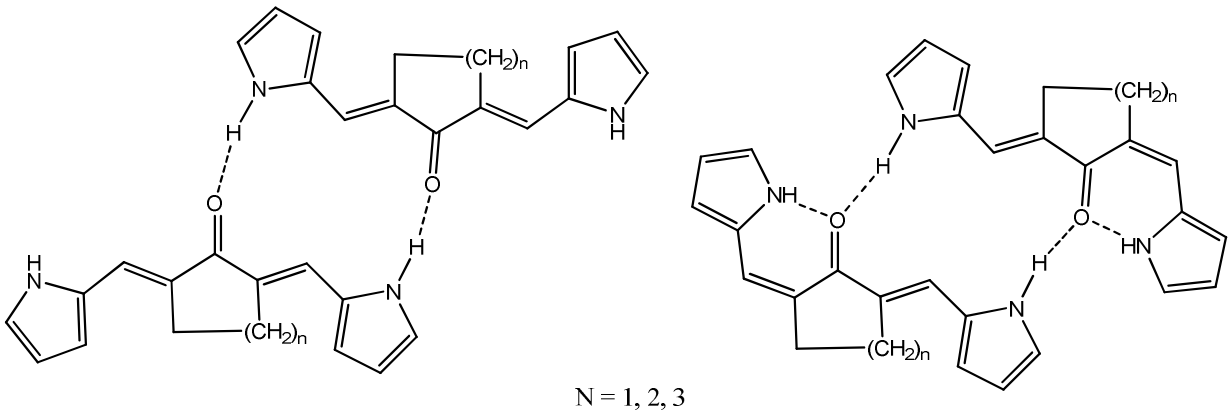

Scheme 7. The structure of dimers of E,E- and Z,E- isomers of compounds **5** – **7**.

The formation of dimers both in gas phase and DMSO solution occurs with a significant energy gain with respect to separate monomers. In the case of dimerization of the Z,E isomers the intramolecular H-bonds N–H···O are elongated relative to the monomers (the H···O distances are 1.786 and 1.759 Å for compound **5**, and 1.778 and 1.732 Å respectively for **6**). The intermolecular N–H···O H-bonds in the Z,E-dimers are longer than in the E,E-isomers (1.880 and 1.852 Å respectively for compound **5** and 1.952 and 1.833 Å respectively for **6**). These results suggest that the intermolecular H-bonding in the Z,E-dimers is weaker than in their E,E-counterparts and are in agreement with the calculated energies of dimerization (Table 4). According to calculations, in the gas phase not only the *Z,E*-monomers but also the *Z,E*-dimers are more stable than the

corresponding *E,E*-dimers, the relative stability being decreased from 8.5 to 5.0 and 4.6 kcal/mol on going from the five- to six- and seven-membered ring compounds. However, in DMSO solution (PCM model) the preference of the *Z,E*-dimer over the *E,E*-dimer for the five-membered ring compound decreases from 8.5 to 2.7 kcal/mol, whereas for the six- and seven-membered compounds the *E,E*-dimers become more stable than the *Z,E*-dimers by 0.88 and 0.56 kcal/mol, respectively. We believe that these results are indicative of the shift of the equilibrium *E,E*-dimers ⇆ *Z,E*-dimers to the left on going from the gas phase to a polar medium. While for compound **5** it results only in a decrease of the preference of the *Z,E*- over the *E,E*-dimer, for compounds **6** and **7** it correctly reproduces the experimentally observed preference of the *E,E*-dimers. Moreover, the aforementioned instability of the **6**-Z,Z isomer is in excellent agreement with its structure which does not allows the formation of dimers of any kind.

Table 4. Total energies[a)] (a. u) of isomers of **5, 6, 7**, their relative energies (kcal/mol)[b)], total energies[c)] (a. u.) of dimers and energies of dimerization (kcal/mol)[d)] as a difference between total energies of H-bonded dimers and double total energies of monomers.

Entry	5_E,E	5_Z,E	5_Z,Z
Gas	-764.9194 [a)] (9.6) [b)] (-1529.8687) [c)] (-18.8) [d)]	-764.9283 [a)] (4.1) [b)] (-1529.8823) [c)] (-16.1) [d)]	-764.9348 [a)] (0) [b)]
DMSO	-764.9367 [a)] (3.7) [b)]	-764.9402 [a)] (1.6) [b)]	-764.9427 [a)] (0) [b)]

	(-1529.8909) [c] (-11.0) [d]	(-1529.8952) [c] (-9.3) [d]	
Entry	6_E,E	6_Z,E	6_Z,Z
Gas	-804.2396 [a] (7.3) [b] (-1608.5067) [c] (-17.3) [d]	-804.2476 [a] (2.2) [b] (-1608.5146) [c] (-12.2) [d]	-804.2512 [a] (0) [b]
DMSO	-804.2555 [a] (2.1) [b] (-1608.5278) [c] (-10.5) [d]	-804.2587 [a] (0.1) [b] (-1608.5264) [c] (-5.6) [d]	-804.2589 [a] (0) [b]
Entry	7_E,E	7_Z,E	7_Z,Z
Gas	-843.5503 [a] (9.8) [b] (-1687.1318) [c] (-19.6) [d]	-843.5598 [a] (3.9) [b] (-1687.1392) [c] (-12.3) [d]	-843.5660 [a] (0) [b]
DMSO	-843.5675 [a] (3.8) [b] (-1687.1528) [c] (-11.2) [d]	-843.5710 [a] (1.6) [b] (-1687.1519) [c] (-6.2) [d]	-843.5736 [a] (0) [b]

As follows from ^{1}H NMR data (see above) the strength of intramolecular hydrogen bond in Z,E-moieties of compound **7** is weaker than that of **5** and **6**. The consideration of optimized structures (Table 5) shows that this compound has markedly different geometric parameters: both the NH···O distance (1.823 Å) and dihedral angle N–H–O=C

(15.5°) significantly exceed the corresponding parameters for **5** and **6**. AIM analysis allows to estimate quantitatively the strength of hydrogen bonds in compounds **5**, **6** and **7** as 11.6, 12.0 and 9.2 kcal/mol, respectively.

Upon the formation of dimers, the structure of Z,E-moieties undergoes significant changes, due to formation of bifurcate hydrogen bonds. For compounds **5** and **6** the internal component of the bifurcate bond elongates by 0.03–0.04 Å, and the dihedral angle N–H–O=C increases to 8.4 and 24.9°, respectively. Unexpectedly, the reverse changes are observed for compound **7**: the internal hydrogen bond shortens by 0.039 Å and the dihedral angle diminishes from 15.5 to 0°. The corresponding AIM parameters (Table 4) also show the increase of the hydrogen bond energy. One can suppose that the increasing stability of intramolecular hydrogen bond in the Z,E-dimer of compound **7** is the reason of direct formation of the 7-Z,E-isomer during the synthesis.

The optimized geometries of complexes of **6** with fluoride and acetate anions (Scheme 6) shed light on the difference in experimental behavior with respect to anions. Thus, complexation of acetate anion with both **6-E,E** and **6-Z,E**-isomers leads to complexes **A** and **B**, but does not affect significantly their geometry as compared to free bases, except for elongation of the N–H bond in complex **B** by 0.048 Å, from 1.009 to 1.057 Å, and shortening of the intramolecular NH···O bond from 1.750 to 1.741 Å, corresponding to strengthening hydrogen bond, Scheme 2). The lengths of intermolecular hydrogen bonds with AcO^- ion are 1.643 Å for complex **A** and 1.626 Å for **B**.

On the contrary, more basic fluoride anion abstracts the proton from the free pyrrole ring of the E-moiety, whereas the remaining hydrogen bond in the Z-moiety of complex **D** becomes shorter by 0.026 Å, from 1.750 to 1.723 Å (Scheme 6, complexes **C** and **D**).

These findings are in full agreement with the experiment, both in relation with color variations (no change for acetate and drastic change for fluoride) and with NMR spectral changes (low-filed movement of hydrogen-bonded proton in **6-Z,E**-isomer from 12.8 to 13.74 ppm).

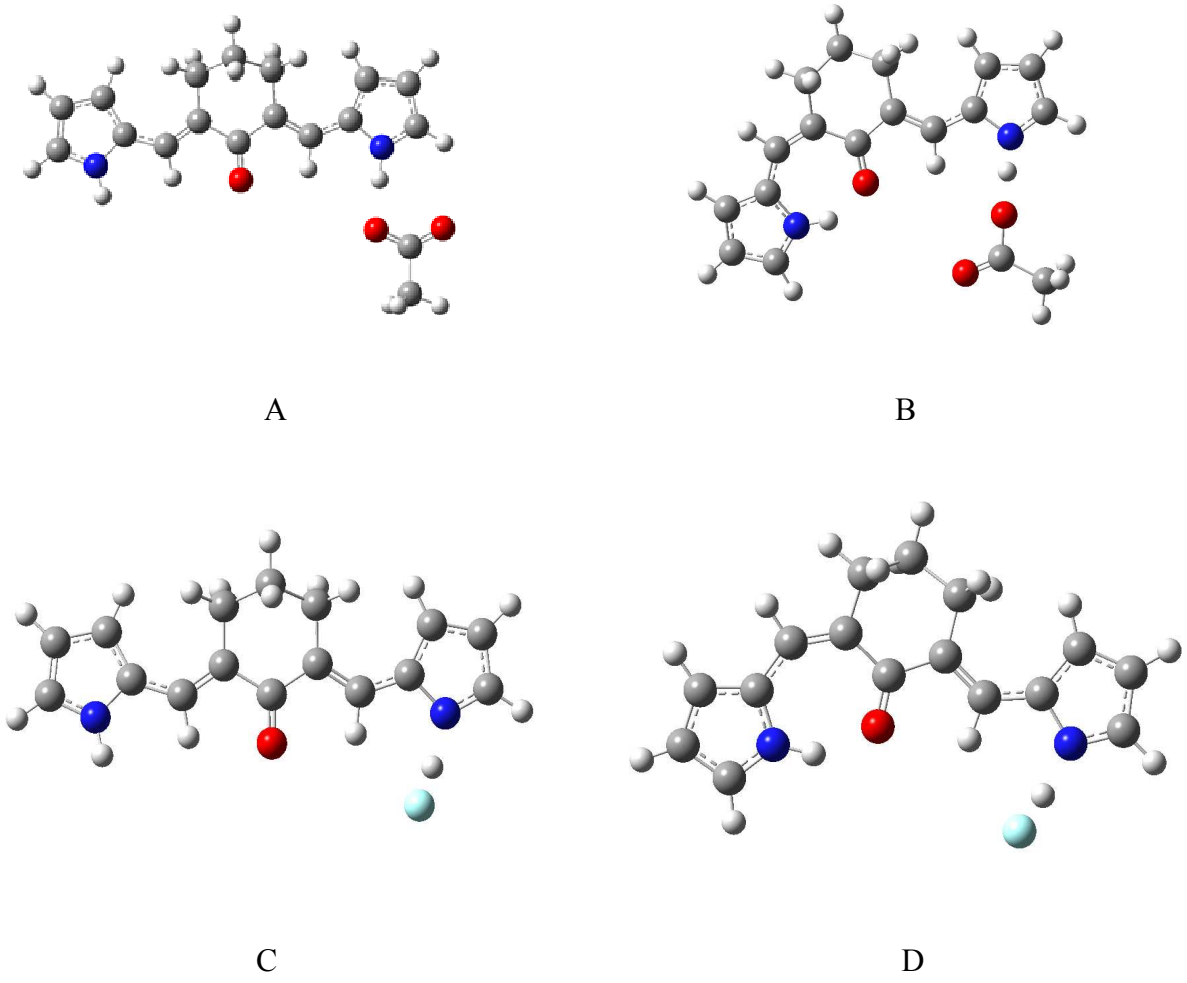

Scheme 8. Optimized geometries of the complexes of 3-E,E- and 3-Z,E- isomers with acetate (A, B) and fluoride (C,D) anions.

Similarly, the optimized structures of O-protonated **6-Z,E-** and **6-E,E**-isomers shows that the hydrogen bond in the first compound significantly weakens (becomes 1.92 Å instead

1.750 in neutral compound. As a result, the **6-E,E-** isomer is more stable by 2.3 kcal/mol which explains the experimentally observed Z,E- to E,E isomerization in the presence of TFA (vide supra).

Table 5. The geometric parameters and AIM estimated energies (E_{HB}) of intra- *and* intermolecular hydrogen bonds N-H**...**O in the molecules of **5**, **6**, **7** and their dimers

	r(NH···O) intramol.,Å	r(NH···O) intermol., Å	φ(NH···O),°	θ(N-H...O=C),°	$E_{(HB)}$ intramol. kcal/mol	$E_{(HB)}$ intermol. kcal/mol
5-Z,E	1.759	-	148.6	0.5	11.6	
6-Z,E	1.750	-	143.2	1.1	12.0	
7-Z,E	1.823	-	141.4	15.5	9.2	
Dimer 5-Z,E	1.786	1.880	147.3	8.4	10.7	6.8
Dimer 6-Z,E	1.790	1.952	141.3	24.9	10.7	5.0
Dimer 7-Z,E	1.784	1.888	139.4	0	10.9	6.8
Dimer 5-E,E	-	1.852	-			7.2
Dimer 6-E,E	-	1.833	-			7.8
Dimer 7-E,E	-	1.840	-			7.8

Experimental Section

Melting points were determined on a Boetius micro hot-stage apparatus and are uncorrected. FTIR spectra of solid compounds **3**–**7** in KBr and of their solutions in CCl_4 and CH_2Cl_2 were recorded. UV-vis spectra for solutions of compounds **4** and **6** in acetonitrile and those with addition of trifluoroacetic acid were recorded. ^{1}H- and ^{13}C-NMR spectra were recorded at working frequencies of 500.13 (^{1}H) and 125.1 (^{13}C) MHz; ^{1}H- and ^{13}C-NMR chemical shifts are reported in parts per million relative to TMS.

Crystal data were collected on a diffractometer with MoK_α radiation (λ = 0.71073 Å) using the φ and ω scans.The structure was solved and refined by direct methods using the SHELX programs set [39]. Data were corrected for absorption effects using the multi-scan method (SADABS). Non-hydrogen atoms were refined anisotropically using SHELX.

For details of the data collection and the structure solution and refinement, see Supplementary data. CCDC 1035672 (**3**), CCDC 1043417 (**4**) and CCDC 1043416 (**6**) contain the supplementary crystallographic data for this paper. These data can be obtained free of charge from the Cambridge Crystallographic Data Centre via www.ccdc.cam.ac.uk/data_request/cif.

Geometry optimization for compounds **3**–**7**, their protonated and deprotonated forms was performed by applying density function theory (DFT) using B3LYP potential and 6-311g(d,p) basis set in the gas phase and in DMSO solution using PCM model. No restrictions were imposed on the geometry optimization. All calculated minima were

verified by frequency calculations; no imaginary frequencies were found. All computations were performed with the Gaussian 03 program package [40].

*2-Pyrrolylmethylidene cycloalkanones **3–6** (general procedure).* To the mixture of 0.02M of cyclic ketone and 2-pyrrolyl-carbaldehyde (1 equiv. for 1-indanone and α-tetralone, 2 equiv. for cyclopentanone and cyclohexanone) in 20 ml of abs. ethanol 2 ml of 4M solution of aqueous potassium hydroxide was added, the mixture was refluxed for 3 h and allowed to stay overnight. The solid precipitate was filtered and washed with cold ethanol. In the case of compounds **3**, **4** and **6** in such a way the crystals suitable for X-ray analysis were obtained. As was mentioned above, the molecules of all these compounds have *E*- or *E,E*-configuration.

(E)-2-((1H-pyrrol-2-yl)methylene)-2,3-dihydro-1H-inden-1-one (**3**). Yellow solid, yield 3.3 g (79%), m.p. 192-194 °C. Anal. Found, %: C, 79.98; H, 4.99; N 6.78. $C_{14}H_{11}NO$. Calcd, %: C, 80.36; H, 5.30; N, 6.69. ^{1}H NMR, 500.13 MHz, $CDCl_3$, δ, ppm: 3.96 (s, 2H); 6.49 (m, 1H); 6.82 (m, 1H); 7.14 (m, 1H); 7.48 (td, *J* = 6.6 and 0.7 Hz, 1H); 7.62 (d, *J* = 7.7 Hz, 1H); 7.66 (td, *J* = 7.3 Hz, 1.1 Hz, 1H); 7.73(t, *J* = 1.8 Hz, 1H); 7.94 (d, *J* = 7.3 Hz, 1H); 9.17 (br., 1H). ^{13}C NMR, 125.13 MHz, $CDCl_3$, δ, ppm: 32.4, 112.0, 114.9, 122.9, 123.6, 124.1, 126.1, 127.6, 129.2, 129.4, 134.1, 138.9, 148.8, 194.0.

(E)-2-((1H-pyrrol-2-yl)methylene)-3,4-dihydronaphthalen-1(2H)-one (**4**). Yellow-orange solid, yield 3.7 g (83%), m.p. 146-147 °C. Anal. Found, %: C, 80.28; H, 5.77; N 6.36. $C_{15}H_{13}NO$. Calcd, %: C, 80.69; H, 5.87; N, 6.27. ^{1}H NMR, 500.13 MHz, $CDCl_3$, δ, ppm: 3.07(t, *J* = 7.3 Hz, 2H); 3.22 (td, *J* = 7.3 and 1.7 Hz, 2H); 6.77(m, 1H); 6.46 (m, 1H) ; 7.33(d, *J* = 8.0 Hz, 1H); 7.10(m, 1H); 7.43 (t, *J* = 7.3, 1H); 7.54 (td, *J* = 7.7 and 1.4 Hz,

1H); 8.06 (t, *J* = 1.7 Hz, 1H); 8,17 (td, *J* = 7.7 and 1.4 Hz, 1H); 9.67 (br, 1H). ^{13}C NMR, 125.13 MHz, $CDCl_3$, δ, ppm: 26.9; 28.0; 111.4; 113.7; 122.0; 127.0; 127.6; 1278; 1281; 128.6; 129.3; 132.9; 133.9; 143.1; 187.5.

(2E,6E)-2,6-bis((1H-pyrrol-2-yl)methylene)cyclopentanone (**5**). Orange solid, yield 4.3 g (90%), m.p. 262 °C Lit.[24] 265-268°C. Found, %: C, 75.20; H, 5.82; N 11.72. $C_{15}H_{14}N_2O$. Calcd, % C 75.61; H 5.92; N 11.76. ^{1}H NMR, 500.13 MHz, DMSO-d_6, δ, ppm: 2.86 (s, 4H); 6.30 (m, 2H); 6.55 (m, 2H); 7.11(m, 2H); 7.32 (br.s, 2H); 11.46 (br, 2H). ^{13}C NMR, 125.13 MHz, DMSO-d_6, δ, ppm: 26.0, 111.6, 114.0, 122.1, 123.3, 129.9, 132.8, 193.9.

(2E,6E)-2,6-bis((1H-pyrrol-2-yl)methylene)cyclohexanone (**6**). Red solid, yield 4.7 g (93%), m.p. 196-199 °C Lit.[24] 204-206°C. Anal. Found, %: C, 76.32; H, 6.31; N 11.17. $C_{16}H_{16}N_2O$. Calcd, %: C, 76.16; H, 6.39; N, 11.10. ^{1}H NMR, 500.13 MHz, $CDCl_3$, δ, ppm: 1.91 (m, 2H); 2.87 (td, *J* = 6.3 and 1.5 Hz, 4H); 6.36 (m, 2H); 6.61 (m, 2H); 6.98 (m, 2H); 7.67 (br. s, 2H); 8.58 (br, 2H). ^{13}C NMR, 125.13 MHz, CD_2Cl_2, δ, ppm: 22.1; 28.2; 111.2; 113.6; 122.6; 126.4; 129.5; 129.8; 187.4.

*2-Pyrrolylmethylene cycloheptanones **7a-7d**.*

To the mixture of 0.45 g of *cycloheptanone* and 0.38 g 2-pyrrolyl-carbaldehyde (2 equiv.) in 20 ml of abs. ethanol 2 ml of 4M solution of aqueous potassium hydroxide was added, the mixture was refluxed for 48 h, allowed to cool, poured into water and extracted with dichloromethane (2x50 ml). The organic phase was washed with water, dried by magnesium sulfate and after solvent evaporation chromatographed on the silica gel column. The eluent for compounds **7a** and **7b** was dichloromethane whereas for **7c** and **7d** – dichloromethane-methanol (4:1)

(Z)-2-((1H-pyrrol-2-yl)methylene)cycloheptanone (**7a**). Yellow solid, yield 0.042 g (8%). ^{1}H NMR, 500.13 MHz, $CDCl_3$, δ, ppm: 1.74 (m, 6H); 2.59 (m, 2H); 2.69 (m, 2H); 6.28 (m, 1H); 6.46 (s, 1H); 6.63 (m, 1H); 6.93 (m, 1H); 12.30 (br., 1H). ^{13}C NMR, 125.13 MHz, $CDCl_3$, δ, ppm: 25.46, 30.81, 31.10, 38.13, 45.11, 110.62, 118.55, 121.61, 125.10, 129.60, 131.74, 205.57. (ESI+)-HRMS: calcd for $C_{12}H_{15}NOH$ $(M + H)^+$ 190.1226, found 190.1222.

(2Z,7E)-2,7-bis((1H-pyrrol-2-yl)methylene)cycloheptanone (**7b**). Red solid, yield 0.084 g (12%). Anal. Found, %: C, 76.56; H, 6.88; N, 10.39; C17H18N2O. Calcd., % C, 76.66; H, 6.81; N, 10.52; ^{1}H NMR, 500.13 MHz, CD_2Cl_2, δ, ppm: 1.84 (m, 4H); 2.49 (m, 2H); 2.67 (m, 2H); 6.28 (m, 1H); 6.34 (m, 1H); 6.45 (m, 1H); 6.55 (m, 1H); 6.63 (br. s, 1H); 6.90 (m, 1H); 6.92 (m, 1H); 7.11 (br. s, 1H); 8.51, (br, 1H); 11.85 (br, 1H). ^{13}C NMR, 125.13 MHz, CD_2Cl_2, δ, ppm: 24.7; 29.2; 30.0; 34.8; 110.2; 110.9; 112.9; 117.0; 120.8; 121.0; 124.6; 129.6; 129.8; 130.2; 131.2; 138.4; 199.0.

(E)-2-((1H-pyrrol-2-yl)methylene)cycloheptanone (**7c**) and *(2E,7E)-2,7-bis((1H-pyrrol-2-yl)methylene)cycloheptanone* (**7d**). Brown solid, yield 0.26 g (50%), the ratio **7c**:**7d** is 4:1.

7c: ^{1}H NMR, 500.13 MHz, $CDCl_3$, δ, ppm: 1.73(m, 2H); 1.79 (m, 4H); 2.70 (m, 2H); 2.76 (m, 2H); 6.31 (m, 1H); 6.58 (m, 1H); 6.93 (m, 1H); 7.48 (br. s, 1H); 9.37, (br, 1H). ^{13}C NMR, 125.13 MHz, $CDCl_3$, δ, ppm: 25.2; 28.4; 28.7; 31.3; 43.4; 111.0; 112.3; 121.2; 126.0; 128.4; 134.8; 205.6.

7d: ^{1}H NMR, 500.13 MHz, $CDCl_3$, δ, ppm: 1.90 (m, 4H); 2.73 (m, 4H); 6.35 (m, 2H); 6.62 (m, 2H); 6.96 (m, 2H); 7.52 (br.s, 2H); 9.52 (br, 2H. ^{13}C NMR, 125.13 MHz, $CDCl_3$, δ,

ppm: 25.1; 27.8; 111.1; 112.7; 121.2; 126.7; 129.1; 135.0; 198.8. ^{1}H NMR spectra are given on Figure S19.

The presence in ^{13}C spectrum (Figure S20) of two signals of aliphatic carbons at 25.1 and 27.8 ppm indicates the symmetric structure of **7d**, whereas five signals at 25.2, 28.4, 28.7, 31.3 and 43.4 ppm correspond to five methylene groups of carbocycle of **7c**. The latter chemical shift value is close to one of α-CH_2 in cycloheptanone [41] and proves the presence of only one pyrrolylidene group in the molecule.

Photochemical isomerization. The solutions of the studied compounds in acetonitrile-d_3 or DMSO-d_6 were irradiated by UV light with 345 nm wavelength during 15 min to 6 h. After irradiation, the isomeric ratio was measured by ^{1}H NMR spectroscopy. The solvent was removed and the Z-isomers were isolated from the residue by column chromatography on silica gel. In the cases of DMSO-d_6 as a solvent, the solution was poured into cold water, the precipitates filtered and chromatographed. In all cases dichloromethane was used as the eluent. Z-Isomers of **3** and **4** were not isolated and their ^{1}H NMR spectra recorded immediately after irradiation. The isolated Z,E-isomers of compounds **5** and **6** were characterized by NMR spectra in CD_2Cl_2 or $CDCl_3$.

(Z)-2-((1H-pyrrol-2-yl)methylene)-2,3-dihydro-1H-inden-1-one (**3Z**). ^{1}H NMR, 500.13 MHz, CD_2Cl_2, δ, ppm: 3.92 (s, 2H); 6.42 (m, 1H); 6.68 (m, 1H); 7.03 (s, 1H); 7.18 (m, 1H); 7.51 (t, 1H); 7.60 (td, *J* = 7.7 and 0.7 Hz, 1H); 7.68 (td, *J* = 7.3 and 1.1 Hz, 1H); 7.92 (d, 1H); 13.43 (br, 1H).

(Z)-2-((1H-pyrrol-2-yl)methylene)-3,4-dihydronaphthalen-1(2H)-one (**4Z**) . ^{1}H NMR, 500.13 MHz, CD_3CN, δ, ppm: 2.95 (m, 2H); 3.07 (m, 2H); 6.36 (m, 1H); 6.64 (m, 1H);

6.96 (s, 1H); 7.14 (m, 1H); 7.44 (td, 1H); 7.39 (d, 1H);7.58 (td, *J* = 7.7 and 1.5 Hz, 1H); 8.16 (dd, *J* = 7.3 and 1.5 Hz, 1H); 12.76 (br, 1H).

(2Z,6E)-2,6-bis((1H-pyrrol-2-yl)methylene)cyclopentanone (**5-Z,E**). ^{1}H NMR, 500.13 MHz, CD_2Cl_2, δ, ppm: 2.96 (m, 4H); 6.29 (m, 1H); 6.43 (m, 1H); 6.52 (m, 1H); 6.55 (m, 1H); 6.76 (s, 1H); 7.11 (m, 1H); 7.12 (m, 1H); 7.41 (t, *J* = 2.2 Hz, 1H); 8.71 (br., 1H); 13.07 (br, 1H).

(2Z,6E)-2,6-bis((1H-pyrrol-2-yl)methylene)cyclohexanone (**6-Z,E**). ^{1}H NMR, 500.13 MHz, $CDCl_3$, δ, ppm: 1.92 (m, 2H); 2.69 (m, 2H); 2.80 (td, *J* = 6.7 and 2.1 Hz, 2H); 6.31 (m, 1H); 6.36 (m, 1H); 6.51 (m, 1H); 6.62 (m, 1H); 6.98 (m, 1H); 6.65 (s, 1H); 7.00 (m, 1H); 7.69 (s, 1H); 8.56 (br, 1H); 13.02 (br, 1H).

Supporting information available. Crystallographic data for compounds **3**, **4**, and **6**, ^{1}H and ^{13}C NMR spectra of compounds **3** – **7** Calculated data (optimized structures of **3** – **7** and their dimers, complexes with anions (for **6**) and cations (for **6**).

References

(1) Perjesi, P.; Takacs-Novak, K.; Rozmer, Z.; Sohar, P.; Bozak, R. E.; Allen, T. M. Central *European Journal of Chemistry,* **2012**, *10*, 1500-1505.

(2) Yamagata, N.; Demizu, Y.; Sato, Y.; Doi, M.; Tanaka, M.; Nagasawa, K.; Okuda, H.; Kurihara, M. *Tetrah. Lett.*, **2011**, *52*, 798-801.

(3) Jonathan R. D.; N. Murthi K.; Adil J. Nazarali, Travis P. Kowalchuk,

Narasimhan Motaganahalli, J. Wilson Quail, Patricia A. Mykytiuk, Gerald F. Audette, Lata Prasad, Pal Perjesi,Theresa M. Allen, C.L. Santos, Jen Szydlowski, Erik De Clercq and Jan Balzarinir, J. Med. Chem. 1999, 42, 1358-1366

(4) Perjesi, P.; Linnanto, J.; Kolehmainen, E.; Osz, E.; Virtanen, E. *J. Mol. Struct.*, **2005**, *740*, 81-89.

(5) Shanmugapriya, S.; Anusha; Aanandhi, M.; Vijey; Ravichandiran, V. *Med. Chem.* **2013**, *2*, 127-135.

(6) Wei, A. C.; Ali, M. A.; Yoon, Y. K.; Ismail, R.; Choon, T.S.; Kumar, R. S.; Arumugam, N.; Almansour, A.I.; Osman, H. *Bioorg. Med. Chem. Lett.* **2012**, *22*, 4930-4933.

(7) Bansal, R.; Narang, G.; Zimmer, C.; Hartmann, R. W. Med. Chem. Res. **2011**, *20*, 661-669.

(8) Vischer, H. F.; Hulshof, J. W.; Hulscher, S.; Fratantoni, S. A.; Verheij, M. H. P.; Victorina, J.; Smit, M. J.; de Esch, I. J. P.; Leurs, R. *Bioorg. Med. Chem*. **2010**, *18*, 675-688.

(9) Karthik, R.; Jasmin, S. R.; Sasikumar, S.; Betanabhatla, K.S.; Christina, A. J. M.; Athimoolam, J.; Saravanan, K. S., *Pharmacology online* **2008**, *2*, 176-191.

(10) Pati, Hari N.; Das, Umashankar; De Clercq, Erik; Balzarini, Jan; Dimmock, Jonathan R., Journal of Enzyme Inhibition and Medicinal Chemistry **2007**, 22(1), 37-42.

(11) Hallgas, B.; Dobos, Zs.; Osz, E.; Hollosy, F.; Schwab, R. E.; Szabo, E. Z.; Eros, D.; Idei, M.; Keri, Gy.; Lorand, T. *Journal of Chromatography B: Analytical Technologies in the Biomedical and Life Sciences,* **2005**, *819*, 283-291.

(12) Dimmock, J. R.; Zello, G.A.; Oloo, E. O.; Quail, J. W.; Kraatz, H.-B.; Perjesi, P.; Aradi, F.; Takacs-Novak, K.; Allen, T. M.; Santos, C. L.; et al. *J. Med. Chem.,* **2002**, *45*, 3103-3111.

(13) Sarjiman S.S., Reksohadiprojio M.S., Hakim L., van der Goot H., Timmerman H.. *Eur. J. Med. Chem.* **1997,** *32*, 625.

(14) Zhang, X ; Fan, X.; Niu, H.; Wang, J. *Green Chem*. **2003***, 5*, 267.

(15) Kawamata, J.; Inoue, K.; Kasatani, H.; Terauchi, H. *Jpn. J. Appl.Phys*. **1992**, *31*, 254.

(16) Gangadhara, K. K. *Macromolecules*, **1993**, *26*, 2995.

(17) Kannan, P.; Gangadhara, K. K.; Kishore, K. *Polymer* **1997**,*38*, 4349.

(18) Kulkarni, S. G.; Panda. S. P. *Combust. Flame* **1980**, *39,* 123.

(19) Vatsadze, S.Z.; Golikov, A.G.; Kriven'ko, A.P.; Zyk, N.V.. *Russ. Chem. Rev*., **2008**, *77*, 661-681.

(20) Evans, D. A.; Nelson, J. V.; Taber, T. R. (1982) *Stereoselective Aldol Condensations*, in: *Topics in Stereochemistry*, v. 13 (N. L. Allinger, E. L. Eliel and S. H. Wilen, eds), John Wiley & Sons, Inc., Hoboken, NJ, USA.

(21) Heathcock, C. H. The aldol addition reaction, Edited by Morrison, James D. *Asymmetric Synth.* **1984**, *3*, 111-212.

(22) Palomo, C.; Oiarbide, M.; Garcia, J. M. *Chem. Soc. Rev*., **2004**, *33*, 65-75.

(23) Dhar D.N. *The chemistry of chalcones and related compounds*, JohnWiley and Sons, New York, 1981, 168.

(24) Braga, S. F. P.; Alves, E. V. P.; Ferreira, R. S.; Fradico, J. R. B.; Lage, P. S.; Duarte, M. C.; Ribeiro, T. G.; Junior, P. A. S.; Romanha, A. J.; Tonini, M. L.; et al. *Eur. J. Med. Chem.* **2014**, *71*, 282-289.

(25) Sigalov, M.; Shainyan, B.; Chipanina, N.; Ushakov, I.; Shulunova, A. *J. Phys. Org. Chem*. **2009**, *22*, 1178-1187.

(26) Sigalov, M. V.; Shainyan, B. A.; Chipanina, N. N.; Oznobikhina, L. P. *J. Phys. Chem. A*., **2013**, *117*, 11346-11356.

(27) Schuster D.I. The photochemistry of enones. In: Patai S, Rappoport Z (eds) The chemistry of enones. John Wiley and Sons, Chichester, **1989**, p 623;

(28) Iwata S.; Nishino T.; Nagata N.; Satomi Y.; Nishino H.; Shibata S. *Biol. Pharm. Bull*., **1997**, *20*, 1266-70.

(29) Perjési, *P.*; *Monatsh. Chem.*, **2015**, 146(8), 1275-81

(30) King N.R.; Whale E.A.; Davis F.J.; Gilbert A.; Mitchell G.R. *J. Mater. Chem*., **1997**, *7*, 625-630.

(31) *Hydrogen Bonding and Transfer in the Excited State*. Han,K.-L.; Zhao, G.-J. Eds. Vol. 1, Wiley, UK, 2011.

(32) Bertolasi, V. ; Gilli, P.; Ferretti, V.; Gilli, G.; Vaughan, K. *New J. Chem.* **1999**, *23*, 1261–1267.

(33) Chipanina, N. N.; Turchaninov, V. K.; Vorontsov, I. I.; Antipin, M. Yu.; Stepanova, Z. V.; Sobenina, L. N.; Mikhaleva, A. I.; Trofimov, B. A. *Russ. Chem. Bull. Engl. Transl.*, **2002**, *51*, 111–116.

(34) Ucak-Astarlioglu , M. G.; Connors, R. E. *J. Phys. Chem. A*, **2005**, *109*, 8275-8279.

(35) Freiberg, W.; Roth, H.; Rautenberg, Ute; Kroeger, C. F. *J. Prakt. Chem.*, **1989**, *331*, 431-438.

(36) Sigalov, M. V.; Schmidt, E. Yu.; Trofimov, A. B.; Trofimov, B. A. *J. Org. Chem.* **1992**, *57*, 3934-3938;

(37) Sigalov, M.V.; Trofimov, A. B.; Schmidt, E. Yu.; Trofimov, B. A. *J. Phys. Org. Chem*. **1993**, *6*, 471-477.

(38) E. S. Stern, C. J. Timmons, *Gillam and Stern's introduction to electronic absorption spectroscopy in organic chemistry*, Edward Arnold LTD London, 1970.

(39) Sheldrick G.M. *Acta Cryst*., **2008**, *A64*, 112 – 122.

(40) Gaussian 03, Revision B.05. M. J. Frisch, G. W. Trucks, H. B. Schlegel, G. E. Scuseria, M. A. Robb, J. R. Cheeseman, J. A. Montgomery, Jr., T. Vreven, K. N. Kudin, J. C. Burant, J. M. Millam, S. S. Iyengar, J. Tomasi, V. Barone, B. Mennucci, M. Cossi, G. Scalmani, N. Rega, G. A. Petersson, H. Nakatsuji, M. Hada, M. Ehara, K. Toyota, R. Fukuda, J. Hasegawa, M. Ishida, T. Nakajima, Y. Honda, O. Kitao, H. Nakai, M. Klene, X. Li, J. E. Knox, H. P. Hratchian, J. B. Cross, C. Adamo, J. Jaramillo, R. Gomperts, R. E. Stratmann, O. Yazyev, A. J. Austin, R. Cammi, C. Pomelli, J. W. Ochterski, P. Y. Ayala, K. Morokuma, G. A. Voth, P. Salvador, J. J. Dannenberg, V. G. Zakrzewski, S. Dapprich, A. D. Daniels, M. C. Strain, O. Farkas, D. K. Malick, A. D. Rabuck, K. Raghavachari, J. B. Foresman, J. V. Ortiz, Q. Cui, A. G. Baboul, S. Clifford, J. Cioslowski, B. B. Stefanov, G. Liu, A. Liashenko, P. Piskorz, I. Komaromi, R. L. Martin, D. J. Fox, T. Keith, M. A. Al-Laham, C. Y. Peng, A. Nanayakkara, M. Challacombe, P. M. W. Gill, B. Johnson,

W. Chen, M. W. Wong, C. Gonzalez, and J. A. Pople, Gaussian, Inc., Pittsburgh PA, 2003.

(41) H.-O. Kalinowski, S. Berger, S. Braun. *Carbon-13 NMR spectroscopy*, 1997, Wiley, p.268.